Capacity Bounds for Cooperative Diversity

Anders Høst-Madsen, *Senior Member, IEEE*

***Abstract*—In a cooperative diversity network, users cooperate to transmit each others' messages; to some extent nodes therefore collectively act as an antenna array and create a virtual or distributed multiple-input multiple-output (MIMO) system. In this paper, upper and lower bounds for the information-theoretic capacity of four-node *ad hoc* networks with two transmitters and two receivers using cooperative diversity are derived. One of the gains in a true MIMO system is a multiplexing gain in the high sisgnal-to-noise ratio (SNR) regime, an extra factor in front of the log in the capacity expression. It is shown that cooperative diversity gives no such multiplexing gain, but it does give a high SNR additive gain, which is characterized in the paper.**

***Index Terms*—Channel capacity, cooperative diversity, Gaussian interference channel, multiple-input multiple-output (MIMO) systems, multiplexing gain, wireless networks.**

I. Introduction

WIRELESS *ad hoc* networks consist of a number of terminals (in the following referred to as nodes) communicating with each other on a peer-to-peer basis without the assistance of a wired network or planned infrastructure. The communication between nodes might take place through several intermediate nodes, creating a multihop network. Wireless *ad hoc* networks have many applications, both commercial and military: wireless local-area networks (LANs) (e.g., IEEE 802.11 [1], [2]), home networks (e.g., HomeRF [3]), device networks (e.g., Bluetooth [4]), sensor and sensor-actuator networks [5].

A limitation to wireless *ad hoc* networks is that for large networks the capacity (bits per second) per node goes to zero as $\frac{1}{\sqrt{N}}$ [6], where N is the number at nodes, i.e., the asymptotic capacity is zero. Additional limitations to performance, also for small networks, are the impairments of the wireless channel: fading, multipath, shadowing, path loss, and interference.

One solution to the above problems is to use multiple antennas at the transmitters and/or receivers (resulting in multiple-input multiple-output (MIMO) systems), an area of research initiated by the papers [7]–[11]. The benefits include an increased capacity—roughly proportional to the minimum of the number of receive and transmit antennas [7], [8]—a robustness to fading and shadowing, i.e., diversity, and decreased interference among different transmissions. To be efficient, however, antennas need to be spaced at least $\lambda/4$ apart, where λ is the wavelength. For many terminals this means that only one or two antennas are realistic. In addition, even for $\lambda/4$ spaced antennas different paths might not be independent, in particular when considering shadowing, and the gain might therefore be less than predicted.

Manuscript received May 24, 2004; revised June 28, 2005. This work was supported in part by the National Science Foundation under Grant CCR–0329908. The material in this paper was presented in part at the IEEE International Symposium on Information Theory, Chicago, IL, Jun./Jul. 2004.

The author is with the Department of Electrical Engineering, University of Hawaii, Honolulu, HI 96822 USA (e-mail: madsen@spectra.eng.hawaii.edu).

Communicated by M. Médard, Associate Editor for Communications.

Digital Object Identifier 10.1109/TIT.2006.871576

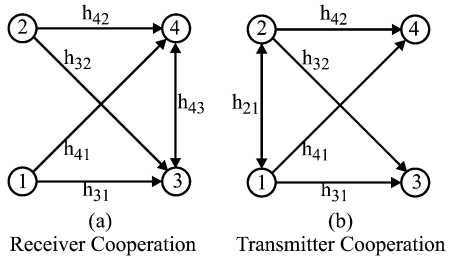

Fig. 1. Channel models for the four-node cooperative channel considered. The desired transmission is $1 \rightarrow 3$ and $2 \rightarrow 4$. The coefficients h_{ij} are channel gains.

The solution considered in this paper is *cooperative diversity*. The basic idea is that several nodes, each with one antenna, form a kind of coalition to cooperatively act as a large transmit or receive array. When terminals cooperate as a transmit array, they first exchange messages and then cooperatively transmit those messages as a multiantenna broadcast transmitter; similarly for receive cooperation. The channel therefore shares characteristics with the MIMO channel, such as diversity.

Cooperative diversity for wireless networks was first investigated by Sedonaris *et al.* in [12]–[15] for cellular networks and by Laneman *et al.* in [16]–[20] for *ad hoc* networks. The idea has also previously been explored in a general information theory context in [21], [22]. Since the nodes can cooperate by relaying each others' messages, cooperative diversity is also related to the relay channel (a few references are [23]–[27]). However, the presence of multiple sources introduces interference into the system, and it therefore has fundamental differences with a single source relay network.

This paper considers the networks in Fig. 1. Node 1 transmits to node 3 and node 2 to node 4. Either receivers (sources) or transmitters (destinations) can cooperate by listening to the transmission and then assist the transmission of the other nodes. All links are wireless links. The objective of the paper is to calculate inner and outer bounds for the Shannon capacity of the two networks in Fig. 1.

This paper builds on previous results obtained in the conferences papers [28], [29] for transmitter cooperation and [30] for receiver cooperation.

A key question is what kind of rate gain can be obtained by cooperation. In this paper, we will mainly focus on how cooperation can aid in overcoming the limitations of interference. It is therefore natural to focus on the high signal-to-noise (SNR) regime, as this is where the capacity is interference limited. In the high-SNR region, there are two possible gains: a multiplexing gain and an additive gain. Let the sum-rate capacity as a function of the noise power σ^2 be $C_s(\sigma^2)$. The *multiplexing*

factor (also called multiplexing gain or degrees of freedom) [31] is then defined by

$$m = \lim_{\sigma^2 \to 0} \frac{C_s(\sigma^2)}{\log(\sigma^{-2})} \tag{1}$$

and the high SNR offset by

$$a = \lim_{\sigma^2 \to 0} C_s(\sigma^2) - m \log(\sigma^{-2}) \tag{2}$$

measured in bits per second per hertz (bits/s/Hz), or

$$a_{\mathrm{dB}} = \frac{10}{m \log 10} a \tag{3}$$

measured in decibels (also called the high-SNR power offset in [32]–[34]).

We will in particular be interested in these limits along the line $R_1 = R_2$ to exclude trivial cases where only one source transmits its message. If both of the limits (1) and (2) exist, it means that the (sum) capacity in the high-SNR region can be approximated by a line with slope m and x-offset a, i.e.,

$$C_s(\sigma^2) \approx m \log(\sigma^{-2}) + a = m \log(10^{a_{\mathrm{dB}}/10} \sigma^{-2}). \tag{4}$$

Clearly, having $m > 1$ is most desirable. If the cooperation were perfect (i.e., $h_{43} = \infty$ in Fig. 1(a) or $h_{21} = \infty$ in Fig. 1(b), for example, by a wired connection) receiver cooperation would reduce to a two-user multiple-access channel (MAC) with two antennas at the receiver (base station) and transmitter cooperation would reduce to a two-antenna broadcast channel with two users. In both cases, it is well known [7], [8], [35] that the multiplexing factor is $m = 2$ except in degenerate cases, i.e., the system has two virtual channels in parallel. One interesting question is if cooperative diversity also gives $m > 1$. The results in this paper show that this is not the case.[1]

The rest of the paper is organized as follows: Sections II–IV introduce various preliminaries, Section V develops inner and outer bounds for receiver cooperation, Section VI inner and outer bounds for transmitter cooperation, and Section VII has numerical results for upper and lower bounds for sum rate. The appendices contain detailed calculations of achievable rates.

Notice that all logarithms throughout the paper are to base 2. Also, we will use $|\cdot|$ for determinant.

II. System Model

Consider the system model in Fig. 1. Node 1 wants to transmit a message $w_1 \in \{1, 2, \ldots, I_1\}$ to node 3, and node 2 a message $w_2 \in \{1, 2, \ldots, I_2\}$ to node 4. Node i (where $i \in \{1, 2, 3, 4\}$ for Fig. 1 (a) and $i \in \{1, 2\}$ for Fig. 1 (b)) transmits the complex-valued baseband symbol stream $x_i'[n]$, $n = 1, \ldots, N$, which is subject to an average power constraint $\frac{1}{N} \sum_{n=1}^{N} |x_i'[n]|^2 \le P_i'$. The transmission between nodes i and j is subject to (slow) flat fading and path loss, which is expressed by a complex-valued channel gain h_{ji}. Channel capacities will be evaluated for fixed channel gains h_{ji}. The received signal at node j (where $j \in \{1, 2\}$ for Fig. 1 (a) and $j \in \{1, 2, 3, 4\}$ for Fig. 1 (b)) is $y_j'[n]$, which is subject to independent and identically distributed (i.i.d.) circular, complex-valued additive Gaussian noise

[1]This result has been extended to arbitrary cooperation in a 4-node network in [36].

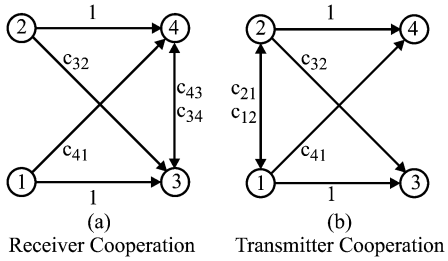

Fig. 2. Normalized channel models.

with power σ_j^2. Each transmitting node has an encoder function f_i^n which maps messages and/or *past* received signals to transmitted signals

$$x_i'[n] = f_i^n\left(w_i, y_i'[n-1], \ldots, y_i'[1]\right). \tag{5}$$

The *rate* for transmission from node i is $R_i = \frac{\log I_i}{N}$. A rate pair (R_1, R_2) is achievable if there exists a sequence of codes so that the average probability of error goes to zero as $N \to \infty$. The capacity region is the closure of the set of achievable rate pairs [37, Sec. 14.3].

At the symbol level, the channel model for Fig. 1(a) is given by

$$y_3'[n] = h_{31} x_1'[n] + h_{32} x_2'[n] + h_{43} x_4'[n] + z_3'[n] \tag{6}$$
$$y_4'[n] = h_{41} x_1'[n] + h_{42} x_2'[n] + h_{43} x_3'[n] + z_4'[n]. \tag{7}$$

For ease of notation and to more clearly evaluate the influence of different parameters, we will normalize this channel model as follows to an equivalent channel (consistent with the literature on the interference channel [38]):

$$\frac{y_3'[n]}{\sigma_3} = \underbrace{\frac{h_{31} x_1'[n]}{\sigma_3}}_{x_1[n]} + \underbrace{\frac{h_{32}\sigma_4}{h_{42}\sigma_3}}_{c_{32}} x_2[n] + \frac{h_{43}}{\sigma_3} x_4'[n] + z_3[n] \tag{8}$$

$$\frac{y_4'[n]}{\sigma_4} = \underbrace{\frac{h_{41}\sigma_3}{h_{31}\sigma_4}}_{c_{41}} x_1[n] + \underbrace{\frac{h_{42} x_2'[n]}{\sigma_4}}_{x_2[n]} + \frac{h_{43}}{\sigma_4} x_3'[n] + z_4[n]. \tag{9}$$

Or

$$\begin{aligned} y_3[n] &= x_1[n] + c_{32} x_2[n] + c_{34} x_4[n] + z_3[n] \\ y_4[n] &= c_{41} x_1[n] + x_2[n] + c_{43} x_3[n] + z_4[n] \end{aligned} \tag{10}$$

shown in Fig. 2(a). Here, $E[|z_3[n]|^2] = E[|z_4[n]|^2] = 1$ and the power constraint $P_1 = |h_{31}|^2 \sigma_3^{-2} P_1'$ and $P_2 = |h_{42}|^2 \sigma_4^{-2} P_2'$.

The channel model for Fig. 1(b) can be described by

$$\begin{aligned} y_1'[n] &= h_{12} x_2'[n] + z_1'[n] \\ y_2'[n] &= h_{12} x_1'[n] + z_2'[n] \\ y_3'[n] &= h_{31} x_1'[n] + h_{32} x_2'[n] + z_3'[n] \\ y_4'[n] &= h_{42} x_2'[n] + h_{41} x_1'[n] + z_4'[n]. \end{aligned} \tag{11}$$

This can similarly be normalized to the model

$$\begin{aligned} y_1[n] &= c_{12} x_2[n] + z_1[n] \\ y_2[n] &= c_{21} x_1[n] + z_2[n] \\ y_3[n] &= x_1[n] + c_{32} x_2[n] + z_3[n] \\ y_4[n] &= x_2[n] + c_{41} x_1[n] + z_4[n]. \end{aligned} \tag{12}$$

In the synchronous channel model, it is assumed that all nodes have complete channel state information (CSI), i.e., each node knows the instantaneous values (magnitudes and phases) of all h_{ij}. It is furthermore assumed that all nodes are perfectly synchronized down to the carrier level. It is relatively straightforward to obtain symbol (timing) synchronization between different nodes; however, carrier synchronization requires phase-locking separated microwave oscillators, which is very challenging in practical systems [39]. In light of this observation, we also consider the asynchronous channel model in which a random phase offset θ_i, due to oscillator fluctuations, is added to the transmitted signal at node i. The received signal model (10) is then replaced by

$$\begin{aligned} y_3[n] &= x_1[n] + c_{32}e^{j(\theta_2[n]-\theta_1[n])}x_2[n] \\ &\quad + c_{43}e^{j(\theta_4[n]-\theta_1[n])}x_4[n] + z_3[n] \\ y_4[n] &= c_{41}e^{j(\theta_1[n]-\theta_2[n])}x_1[n] + x_2[n] \\ &\quad + c_{43}e^{j(\theta_3[n]-\theta_2[n])}x_3[n] + z_4[n]. \end{aligned} \tag{13}$$

We model $\theta_i[n]$ as random and ergodic, uniformly distributed in $[0, 2\pi)$. We further assume that only the destinations know (i.e., can estimate and track) $\theta_i[n]$. The random phases can be included in the coefficients c_{ij}, so that this model is equivalent to the model (10), but with c_{ij} having a random, unknown phase. Similarly the model (12) is changed to

$$\begin{aligned} y_1[n] &= c_{12}e^{j\theta_2[n]}x_2[n] + z_1[n] \\ y_2[n] &= c_{21}e^{j\theta_1[n]}x_1[n] + z_2[n] \\ y_3[n] &= x_1[n] + c_{32}e^{j(\theta_2[n]-\theta_1[n])}x_2[n] + z_3[n] \\ y_4[n] &= x_2[n] + c_{41}e^{j(\theta_1[n]-\theta_2[n])}x_1[n] + z_4[n] \end{aligned} \tag{14}$$

where the random phases again can be included in the coefficients c_{ij}.

In the asynchronous model with receiver cooperation, the transmitters need not have any CSI, except the rate at which they should transmit. The receivers need to know all magnitudes $|h_{ij}|$, but not their phases (for transmission). In the asynchronous model with transmitter cooperation, the transmitters need to know all magnitudes $|h_{ij}|$. Thus, receiver cooperation is suitable for systems with simple transmitters such as sensor nodes.

III. Coding Techniques

In this section, we will review the coding methods used to derive achievable rates, as these are used repeatedly.

A. Multiplexed Coding

A codeword can convey different kinds of information depending on the side information the receiver has. Suppose the transmitter wants to transmit two messages $w_1 \in \{1, \dots 2^{nR_1}\}$ and $w_2 \in \{1, \dots 2^{nR_2}\}$. The transmitter makes a table with 2^{nR_1} rows and 2^{nR_2} columns, and assigns a random (Gaussian) code to each entry in the table, denoted $X(w_1, w_2)$. A receiver can decode both w_1 and w_2 if the channel capacity $C > R_1 + R_2$. If it knows w_1, however, it can decode w_2 if $C > R_2$ simply by only searching the row corresponding to w_1, and similarly if it knows w_2. This can be extended to more messages, and this simple technique plays a key role in cooperation.

B. Block Markov Coding and Decode–Forward

Block Markov coding was introduced in [23] for the relay channel. A message is divided into M blocks, and each block is encoded separately. Let message i be divided into the blocks $w_i[1], \dots, w_i[M]$. To outline the idea, consider a relay channel, for example Fig. 2 with transmission between nodes 1 and 3 and with node 2 acting as relay (and node 4 removed). Node 1 transmits the sequence of blocks $X_1[1](w_1[1]), \dots, X_1[M](w_1[M])$, where $X_1[i]$ is a codeword from a random Gaussian codebook.[2] The relay node decodes $w_1[i]$ during block i, which is possible with zero error probability if $R_1 \leq \log(1 + |c_{21}|^2 P_1)$. It then transmits $w_1[i]$ during block $i + 1$ using the random Gaussian codebook $X_2(w_1)$, i.e., it transmits the sequence $0, X_2[2](w_1[1]), \dots, X_2[M + 1](w_1[M])$. The whole transmission of M messages therefore uses $M + 1$ blocks, but as observed in [23], when $M \to \infty$ this still gives a rate of R. We will call this signaling method *decode–forward*. Now consider decoding at node 3. In [23], list decoding was used for decoding. This was simplified in [40] using the backward decoding introduced in [21] and achieving the same rate as in [23], but actually a simpler argument based on parallel (Gaussian) channels due to Valenti [41] will work. In multi-source networks, it seems that parallel channel arguments and backward decoding sometimes give different results, and we will use both arguments.

In *parallel channel* decoding, the decoding at the destination is forward in time. Suppose that block i has been received, and that $w_1[i-2]$ has been decoded error-free. Then $X_2[i-1](w_1[i-2])$ is known. Based on the received signal, node 3 can then form

$$\begin{aligned} \begin{bmatrix} Y_3[i] \\ Y_3'[i-1] \end{bmatrix} &= \begin{bmatrix} Y_3[i] \\ Y_3[i-1] - c_{32}X_2[i-1](w_1[i-2]) \end{bmatrix} \\ &= \begin{bmatrix} X_1[i](w_1[i]) + c_{32}X_2[i](w_1[i-1]) + Z_3[i] \\ X_1[i-1](w_1[i-1]) + Z_3[i-1] \end{bmatrix}. \end{aligned} \tag{15}$$

Consider decoding of $w_1[i-1]$. The signal $X_1[i](w_1[i])$ can be considered part of the background noise. The two signals $(Y_3[i], Y_3'[i-1])$ then form a parallel Gaussian channel with fixed power allocation for transmission/decoding of $w_1[i-1]$, and the rate bound is therefore simply the sum of the rates in each channel [37, Sec. 10.4]. In this case we get

$$\begin{aligned} R_1 &\leq \log\left(1 + \frac{|c_{32}|^2 P_2}{1 + P_1}\right) + \log(1 + P_1) \\ &= \log\left(1 + P_1 + |c_{32}|^2 P_2\right). \end{aligned}$$

This argument can straightforwardly be extended to more complex channels. We will mention that if we consider a MAC. the rate bounds for the MAC parallel Gaussian channel is simply the sum of the MAC bounds for each of the channels.

In *backward decoding* [21], the source instead transmits

$$X_1[1](0, w_1[1]), X_1[2](w_1[1], w_1[2]), \dots, X_1[M](w_1[M], 0)$$

where $X_1[i](w_1[i-1], w_1[i])$ is encoded using multiplexed coding. The relay still decodes forward: suppose that it has

[2]We denote the sequence of symbols transmitted or received during a block by capital letters with each single symbol in lower case

decoded $w_1[i-1]$ in block $i-1$. It can then decode $w_1[i]$ from $X_1[i](w_1[i-1], w_1[i])$ if $R_1 \leq \log(1+|c_{21}|^2 P_1)$. The received signal at the destination in block i is

$$Y_3[i] = X_1[i](w_1[i-1], w_1[i]) + c_{32} X_2[i](w_1[i-1]) + Z_3[i]. \tag{16}$$

The decoding starts from the last block and proceeds backward to the first block: suppose the source has decoded $w_1[i]$. It can then decode $w_1[i-1]$ from $Y_3[i]$ if

$$R_1 \leq \log\left(1 + P_1 + |c_{32}|^2 P_2\right)$$

by multiplexed coding arguments.

C. Wyner–Ziv Compression and Compress–Forward

When a cooperating node has received a signal, instead of decoding it, re-encoding it and transmitting the re-encoded message, it can instead amplify and forward the received signal without decoding. As an alternative to simple amplification, it can use source coding with distortion to compress the received signal into an index. This index can then be channel coded and transmitted to the destination. This is called *compress–forward*. The most efficient source coding is Wyner–Ziv coding [42], [43]. When Wyner–Ziv source coding is used, we get the following result for decode–forward coding. We will not prove it here, as it has been used before in other papers [24], [25]. A proof can be made along the lines of the proof of Proposition 3 in [24]

Proposition 1: Suppose that receivers 1 and 2 receive the i.i.d. circular complex Gaussian signals $y_1[n]$ and $y_2[n]$, respectively, and suppose that the signal $y_2[n]$ is compressed with a rate R using Wyner–Ziv source coding and forwarded to node 1. In the limit $N \to \infty$, this system is equivalent to a system where receiver 1 has two antennas that receive the signals

$$\begin{bmatrix} y_1[n] \\ y_2[n] + z_w[n] \end{bmatrix} \tag{17}$$

where $z_w[n]$ is i.i.d. circular Gaussian noise called the *compression noise*, independent of $y_1[n]$ and $y_2[n]$, and with power

$$\sigma_w^2 = \frac{E\left[|y_2[n]|^2\right] E\left[|y_1[n]|^2\right] - |E\left[y_1[n] y_2[n]^*\right]|^2}{(2^R - 1) E\left[|y_1[n]|^2\right]}. \tag{18}$$

Corollary 1: If $y_2[n]$ in Proposition 1 contains an interference signal $s[n]$ which is completely known by receiver 1, then Proposition 1 is true with $y_2[n]$ everywhere replaced by $y_2[n] - s[n]$.

D. Costa's "Writing on Dirty Paper"

Consider an additive white Gaussian noise (AWGN) channel with interference. The received signal is

$$y[n] = x[n] + s[n] + z[n] \tag{19}$$

where x is the transmitted signal with power P, s the interference with power Q, and z white Gaussian noise (WGN) with power 1. If the receiver knows the interference perfectly the channel capacity is the same as if there was no interference, $C = \log(1+P)$. In [44], Costa proved that if the receiver does not know the interference, while on the other hand the transmitter knows the interference perfectly (noncausally), then the rate is still $C = \log(1+P)$. This is possible through "binning" at the transmitter, and has become known as "dirty-paper coding." This was used in [35] to find the sum capacity of a two-antenna broadcast channel, and it was recently proved to give the full capacity region of a multiple-antenna broadcast channel [45].

When needed, we will use the notation $X(w, s)$ if X is dirty-paper coded with the message w and s or a known complex multiple of s as interference.

IV. The Gaussian Interference Channel

If there is no cooperation in the channel in Fig. 1, the channel is the Gaussian interference channel [46], [38], [37], and we will use this channel for baseline comparison. We will therefore summarize a few results on outer bounds and achievable rates. First, the outer bounds

$$R_1 \leq \log(1+P_1) \tag{20}$$

$$R_2 \leq \log(1+P_2) \tag{21}$$

always apply. If $|c_{41}| > 1$, we also have an upper bound [46], [47] at node 3

$$R_1 + R_2 \leq \log\left(1 + P_1 + |c_{32}|^2 P_2\right) \tag{22}$$

with a symmetric bound at node 4 if $|c_{32}| > 1$. If both $|c_{41}| > 1$ and $|c_{32}| > 1$, this in fact gives the exact capacity region [46], [47]. If $|c_{41}| \leq 1$, we have the following outer bound [48]–[50] (slightly restated):

$$R_2 \leq \log\left(\frac{1 + |c_{41}|^2 P_1 + P_2}{|c_{41}|^2 2^{R_1} + 1 - |c_{41}|^2}\right) \tag{23}$$

with a symmetric bound for R_1 if $|c_{32}| \leq 1$.

For the achievable rate, [46] gives a rate region, which however is very complicated to evaluate. We will only consider simple coding: either the channel uses time-division multiple access (TDMA), or each transmitter node encodes using independent Gaussian codes, and each receiver decodes this using either joint decoding (where it jointly decodes the transmission of both source nodes) or individual decoding, where it considers the undesired transmission as part of the Gaussian noise. This gives in total five different combinations of coding, and we use the maximum over these as the achievable rate. As will be seen from numerical results later, this gives an achievable rate close to the upper bound.

To find the performance characteristics in the high-SNR region, we recall that we are considering the normalized system model, where transmit powers have been normalized by the noise power. To find the high SNR limit we therefore make this explicit by letting $P_1 = \sigma^{-2} P_1'$, $P_2 = \sigma^{-2} P_2'$ (where P_1', and P_2' are constants), and then let $\sigma^2 \to 0$. First consider the case $|c_{41}| > 1$. For σ^2 small enough, the bound (22) on the sum rate is smaller than the sum of the bounds (20) and (21). The sum rate is therefore bounded by $\log\left(1 + \sigma^{-2}\left(P_1' + |c_{32}|^2 P_2'\right)\right)$. In the limit $\sigma^2 \to 0$, it is then clear that the multiplexing factor $m \leq 1$ and that the high-SNR offset is bounded by $\log(P_1' + |c_{32}|^2 P_2')$.

For $|c_{41}| < 1$, notice that the bound on $R_1 + R_2$ obtained from (23) by adding R_1 on both sides of the inequality

$$R_1 + R_2 \leq R_1 + \log\left(\frac{1 + |c_{41}|^2 P_1 + P_2}{|c_{41}|^2 2^{R_1} + 1 - |c_{41}|^2}\right) \tag{24}$$

is an increasing function R_1. If we therefore insert the upper bound (20) in (24), we get the following bound on the sum rate:

$$R_1 + R_2 \leq \log\Bigg(1 + \sigma^{-2}P_1' + \frac{\sigma^{-2}P_2'}{|c_{41}|^2\sigma^{-2}P_1' + 1} + \frac{\sigma^{-4}P_1'P_2'}{|c_{41}|^2\sigma^{-2}P_1' + 1}\Bigg). \tag{25}$$

Again, it is clear from this that $m \leq 1$ and by taking the limit on the right-hand side of this bound subtracted by $\log(\sigma^{-2})$ we get that

$$a \leq \log\left(|c_{41}|^2 P_1' + P_2'\right) - \log\left(|c_{41}|^2\right). \tag{26}$$

The following proposition summarizes these results, removing the primes from the nonnormalized powers for ease of notation

Proposition 2: Unless $|c_{41}| = |c_{32}| = 0$, the multiplexing factor for the interference channel is $m = 1$. If $|c_{32}| > 1$ and $|c_{41}| > 1$, the high-SNR offset is

$$a = \min\left\{\log\left(P_1 + |c_{32}|^2 P_2\right), \log\left(|c_{41}|^2 P_1 + P_2\right)\right\} \tag{27}$$

otherwise, the high-SNR offset is upper-bounded by

$$a \leq \min\Bigg\{\log\left(P_1 + |c_{32}|^2 P_2\right) - \log\min\left\{|c_{32}|^2, 1\right\}, \log\left(|c_{41}|^2 P_1 + P_2\right) - \log\min\left\{|c_{41}|^2, 1\right\}\Bigg\}. \tag{28}$$

The best achievable offset is in all cases given by (27).

The last statement shows that (as far as is known to the author) there is no way to take advantage of the fact that the interference is weak in the high-SNR regime without cooperation. The best rate is obtained by doing joint decoding, which has poor performance for weak interference. As will be seen later (cf. Fig. 8) cooperation, on the other hand, can take advantage of the fact that interference is weak.

V. Receiver Cooperation

In receiver cooperation, the two receiver nodes, 3 and 4, cooperate on receiving the signal, see Fig. 1(a). We will first derive outer bounds on the capacity region, and then a number of different coding methods for achievable rate. We will show that one of these coding methods comes within 3 dB of the upper bounds in the high-SNR regime.

A. Outer Bound

Applying the max-flow-min-cut theorem [37, Theorem 14.10.1] to the system model results in the following bounds on the rates:

$$R_1 + R_2 \leq I(x_1, x_2; y_3, y_4 | x_3, x_4) \tag{29}$$
$$R_1 \leq I(x_1; y_3, y_4 | x_2, x_3, x_4) \tag{30}$$
$$R_2 \leq I(x_2; y_3, y_4 | x_2, x_3, x_4) \tag{31}$$
$$R_1 \leq I(x_1, x_4; Y_3 | x_2, x_3) \tag{32}$$
$$R_2 \leq I(x_2, x_3; Y_4 | x_1, x_4) \tag{33}$$

where the variables y_i are governed by the channel model (10). A standard argument shows that these bounds are maximized for (x_1, x_2, x_3, x_4) jointly Gaussian (a detailed argument is similar to the proof of [23, Theorem 5]). By assumption, x_1 and x_2 are independent. Furthermore, by looking at the equations it can be seen that none of the mutual informations will be increased if x_3 and x_4 are dependent, if x_1 and x_3 are dependent, or if x_2 and x_4 are dependent. What remains is a possible dependency between x_1 and x_4 and x_2 and x_3. We express this by

$$|E\left[x_1 x_4^*\right]| = \sqrt{\beta_1 P_1 P_4} \tag{34}$$
$$|E\left[x_2 x_3^*\right]| = \sqrt{\beta_2 P_2 P_3} \tag{35}$$

where $0 \leq \beta_1, \beta_2 \leq 1$. We then get the following bounds:

$$R_1 \leq \log\left(1 + \left(1 + |c_{41}|^2\right)(1 - \beta_1)P_1\right) \tag{36}$$
$$R_2 \leq \log\left(1 + \left(|c_{32}|^2 + 1\right)(1 - \beta_2)P_2\right) \tag{37}$$
$$R_1 \leq \log\left(1 + P_1 + |c_{34}|^2 P_4 + 2\sqrt{\beta_1 |c_{34}|^2 P_1 P_4}\right) \tag{38}$$
$$R_2 \leq \log\left(1 + P_2 + |c_{43}|^2 P_3 + 2\sqrt{\beta_2 |c_{43}|^2 P_2 P_3}\right) \tag{39}$$
$$R_1 + R_2 \leq \log\Big(1 + P_1 + |c_{41}|^2 P_1 + |c_{32}|^2 P_2 + P_2 + \left(|c_{32}|^2 |c_{41}|^2 - 2\mathrm{Re}\{c_{41}c_{32}\} + 1\right) P_1 P_2\Big) \tag{40}$$

which should be maximized with respect to β_1 and β_2. For the asynchronous case, using Lemma 1 in [24], it is easily seen that we get

$$R_1 \leq \log\left(1 + P_1 + |c_{41}|^2 P_1\right) \tag{41}$$
$$R_2 \leq \log\left(1 + |c_{32}|^2 P_2 + P_2\right) \tag{42}$$
$$R_1 \leq \log\left(1 + P_1 + |c_{34}|^2 P_4\right) \tag{43}$$
$$R_2 \leq \log\left(1 + P_2 + |c_{43}|^2 P_3\right) \tag{44}$$
$$R_1 + R_2 \leq \log\Big(1 + P_1 + |c_{41}|^2 P_1 + |c_{32}|^2 P_2 + P_2 + \left(|c_{32}|^2 |c_{41}|^2 - 2\mathrm{Re}\{c_{41}c_{32}\} + 1\right) P_1 P_2\Big). \tag{45}$$

The bounds obtained by the max-flow-min-cut are rather loose; for one thing, the multiplexing gain obtained using the bounds is 2. A much stronger bound is the following.

Theorem 1: Consider a system with receiver cooperation. The following bound applies for asynchronous systems:

$$R_1 + R_2 \leq \log\left(1 + |c_{41}|^2 P_1 + P_2 + |c_{43}|^2 P_3\right) + \log\left(\frac{1 + (1 + |c_{41}|^2)P_1}{1 + |c_{41}|^2 P_1}\right) \tag{46}$$

and for synchronous systems

$$R_1 + R_2 \leq \log\Big(1 + |c_{41}|^2 P_1 + P_2 + |c_{43}|^2 P_3 + 2\sqrt{|c_{43}|^2 P_2 P_3 + |c_{43}|^2 |c_{41}|^2 P_1 P_3}\Big) + \log\left(\frac{1 + (1 + |c_{41}|^2)P_1}{1 + |c_{41}|^2 P_1}\right). \tag{47}$$

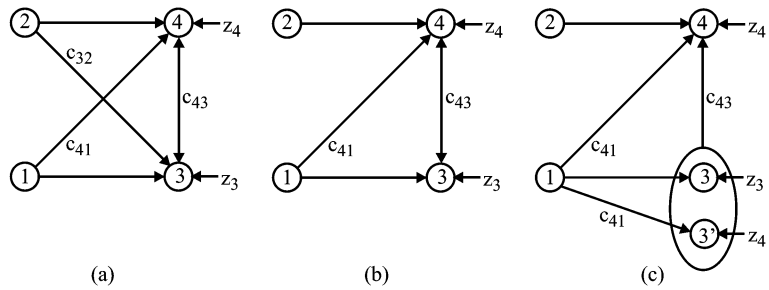

Fig. 3. Channel transformations used in the proof of Theorem 1. All noise variables z_i are independent, and all have power 1.

Proof: The bound is inspired by bounds for the Gaussian interference channel in [48], [50]. We modify the system as indicated on Fig. 3, and we will argue that each step either leads to an equivalent system or a system with a larger capacity region. In the first step, node 3 is given as side information the message w_2, and the link from node 2 to node 3 can therefore be deleted. In the second step, node 3 gets as side information the signal $y_3'[i] = c_{41}x_1[i] + z_4[i]$. With this, knowledge of w_2, and past received signals $y_3[i-1], \dots, y_3[1]$ it can now reconstruct $y_4[i]$, and the link from node 4 to node 3 can then be deleted. We consider upper bounds for the system in Fig. 3(c).

Let $\boldsymbol{y}_j[i] = \{y_j[i], y_j[i-1], \dots, y_j[1]\}$. We can now bound R_1 as follows using the chain rule:

$$nR_1 \le H(\boldsymbol{y}_3[n], \boldsymbol{y}_3'[n]|w_2) - H(\boldsymbol{y}_3[n], \boldsymbol{y}_3'[n]|\boldsymbol{x}_1[n], w_2) + n\epsilon_n \tag{48}$$

$$= \sum_{i=1}^{n} H\left(y_3[i], y_3'[i]|\, \boldsymbol{y}_3[i-1], \boldsymbol{y}_3'[i-1], w_2\right) - \sum_{i=1}^{n} \left(H(z_3[i]) + H(z_4[i])\right) + n\epsilon_n \tag{49}$$

$$= \sum_{i=1}^{n} H\left(y_3[i]|\, y_3'[i], \boldsymbol{y}_3[i-1], \boldsymbol{y}_3'[i-1], w_2\right) + \sum_{i=1}^{n} H\left(y_3'[i]|\, \boldsymbol{y}_3[i-1], \boldsymbol{y}_3'[i-1], w_2\right) - \sum_{i=1}^{n} \left(H(z_3[i]) + H(z_4[i])\right) + n\epsilon_n \tag{50}$$

$$\le \sum_{i=1}^{n} H\left(y_3[i]|\, y_3'[i]\right) + \sum_{i=1}^{n} H\left(y_3'[i]|\, \boldsymbol{y}_3[i-1], \boldsymbol{y}_3'[i-1], w_2\right) - \sum_{i=1}^{n} \left(H(z_3[i]) + H(z_4[i])\right) + n\epsilon_n. \tag{51}$$

Here

$$H\left(y_3[i]|\, y_3'[i]\right) \le \log(2\pi e) + \log E\left[\mathrm{var}[y_3[i]|y_3'[i]]\right] \tag{52}$$

$$= \log(2\pi e) + \log\big(E\big[\mathrm{var}[x_1[i]|c_{41}x_1[i] + z_4[i]]\big] + \mathrm{var}[z_3[i]]\big). \tag{53}$$

By Lemma 1 below

$$E\left[\mathrm{var}[x_1[i]|c_{41}x_1[i] + z_4[i]]\right] \le P_1 - \frac{(|c_{41}|P_1)^2}{|c_{41}|^2P_1 + 1} \tag{54}$$

$$= \frac{P_1}{1 + |c_{41}|^2P_1}. \tag{55}$$

Then

$$\sum_{i=1}^{n} H\left(y_3'[i]|\, \boldsymbol{y}_3[i-1], \boldsymbol{y}_3'[i-1], w_2\right) \ge nR_1 + n\log\left(2\pi e \frac{1 + |c_{41}|^2P_1}{1 + (1 + |c_{41}|^2)P_1}\right) - n\epsilon_n. \tag{56}$$

The rate R_2 can be bounded by

$$nR_2 \le H(\boldsymbol{y}_4[n]) - H(\boldsymbol{y}_4[n]|w_2) + n\epsilon_n. \tag{57}$$

In the asynchronous case, we can bound the first term, using Lemma 1 in [24], by

$$H(\boldsymbol{y}_4[n]) \le n\log(2\pi e) + n\log\left(1 + |c_{41}|^2P_1 + P_2 + |c_{43}|^2P_3\right). \tag{58}$$

In the synchronous case, $H(\boldsymbol{y}_4)$ is maximized by making x_1, x_3, and x_2 dependent. Taking into account that the variables x_1 and x_2 are independent, we can put

$$|E\left[x_2x_3^*\right]| = \sqrt{\beta' P_2P_3} \tag{59}$$

$$|E\left[x_1x_3^*\right]| = \sqrt{(1-\beta')P_1P_3}. \tag{60}$$

Then

$$H(\boldsymbol{y}_4[n]) \le n\log(2\pi e) + n\log\left(1 + \left(|c_{41}|\sqrt{P_1} + |c_{43}|\sqrt{(1-\beta')P_3}\right)^2 + \left(\sqrt{P_2} + |c_{43}|\sqrt{\beta' P_3}\right)^2\right) \tag{61}$$

$$\le n\log(2\pi e) + n\log\Big(1 + |c_{41}|^2P_1 + P_2 + |c_{43}|^2P_3 + 2\sqrt{|c_{43}|^2P_2P_3 + |c_{43}|^2|c_{41}|^2P_1P_3}\Big) \tag{62}$$

where we have maximized with respect to β' in (62).

The second term in (57) can be bounded by

$$H(\boldsymbol{y}_4[n]|w_2) = \sum_{i=1}^{n} H(y_4[i]|\boldsymbol{y}_4[i-1], w_2) \tag{63}$$

$$\geq \sum_{i=1}^{n} H(c_{41}x_1[i] + x_2[i] + c_{43}x_3[i] + z_4[i]|\boldsymbol{y}_4[i-1], w_2, \boldsymbol{x}_2[i], \boldsymbol{x}_3[i]) \tag{64}$$

$$\geq \sum_{i=1}^{n} H(c_{41}x_1[i] + z_4[i]|\boldsymbol{y}_4[i-1], w_2, \boldsymbol{x}_2[i], \boldsymbol{x}_3[i]) \tag{65}$$

$$= \sum_{i=1}^{n} H(y_3'[i]|\boldsymbol{y}_4[i-1], w_2, \boldsymbol{x}_2[i], \boldsymbol{x}_3[i]) \tag{66}$$

$$\geq \sum_{i=1}^{n} H\Big(y_3'[i]|\boldsymbol{y}_4[i-1], w_2, \boldsymbol{x}_2[i], \boldsymbol{x}_3[i], \boldsymbol{y}_3[i-1], \boldsymbol{y}_3'[i-1]\Big) \tag{67}$$

$$= \sum_{i=1}^{n} H\left(y_3'[i]|w_2, \boldsymbol{y}_3[i-1], \boldsymbol{y}_3'[i-1]\right) \tag{68}$$

where we have repeatedly used that conditioning reduces entropy. In (67) and (68), we have used that

$$\boldsymbol{y}_4[i-1] = \boldsymbol{y}_3'[i-1] + \boldsymbol{x}_2[i-1] + c_{43}\boldsymbol{x}_3[i-1],$$

that $\boldsymbol{x}_2[i]$ depends only on w_2, and that $\boldsymbol{x}_3[i]$ depends only on $\boldsymbol{y}_3[i-1]$, $\boldsymbol{y}_3'[i-1]$, and w_2.

Inserting (56) into (68), using (58) or (62) we then get (46) and (47) from (57) by letting $n \to \infty$. □

Lemma 1: For any random variables X and Y with first- and second-order moments

$$E\left[\mathrm{var}[Y|X]\right] \leq E[|Y|^2] - \frac{|E[XY]|^2}{E[|X|^2]}. \tag{69}$$

Proof: First, notice that

$$E\left[\mathrm{var}[Y|X]\right] = E[|Y|^2] - E\left[|E[Y|X]|^2\right]. \tag{70}$$

Second, the Cauchy–Schwartz inequality gives

$$|E[XY]| = |E[XE[Y|X]]| \leq \sqrt{E[|X|^2]}\sqrt{E\left[|E[Y|X]|^2\right]}. \tag{71}$$

Inserting this gives (69). □

From the general upper bound we can easily determine the behavior of receiver cooperation in the high-SNR region. The result is summarized in the following proposition, with arguments as those leading to Proposition 2

Proposition 3: Receiver cooperation gives a multiplexing factor $m = 1$. The high-SNR offset in asynchronous systems is bounded by

$$a \leq \log\left(|c_{41}|^2P_1 + P_2 + |c_{43}|^2P_3\right) + \log\left(1 + |c_{41}|^{-2}\right) \tag{72}$$

and in synchronous systems by

$$a \leq \log\Big(|c_{41}|^2P_1 + P_2 + |c_{43}|^2P_3 + 2\sqrt{|c_{43}|^2P_2P_3 + |c_{41}|^2|c_{43}|^2P_1P_3}\Big) + \log\left(1 + |c_{41}|^{-2}\right). \tag{73}$$

B. Achievable Rate

The cooperative channel is a combination of the interference channel and the relay channel. The coding methods for the cooperative channel are therefore inspired by the coding methods for these two channels. For the interference channel, the two sources use independent Gaussian codebooks and the receivers can either use joint decoding or individual decoding, considering the other signal as noise. In the relay channel, the relay can either use decode–forward or compress–forward [24]. In the cooperative channel combination of these methods with additional twists specific to the cooperative channel give an almost unlimited number of variations. Instead of listing all of these variations, we will concentrate on a selection of methods that illustrate the multiuser (multisource) characteristics of the cooperative channel, as compared to the single-source relay channel, and that are able to achieve rates close to the upper bound, at least in the cases we have explored.

The general idea, in the asynchronous case, is that a receiver node takes its received information, processes it in some way, and forwards it to the other node. We will call this information "cooperation data" (also called "resolution information" in [23]).

1) Compress–Forward Coding: Fig. 4 illustrates compress–forward coding. Node 3 takes its received signal in block i

$$Y_3[i] = X_1(w_1[i]) + c_{32}X_2(w_2[i]) + c_{34}X_4[i] + Z_3[i] \tag{74}$$

compresses it using Wyner–Ziv coding, channel codes it, and transmits it as $X_3[i+1]$, indicated in Fig. 4 with an arrow; similarly for node 4. Notice that decoding does not have to be real time, but can wait until all blocks have been received. There are therefore two possibilities for decoding: forward or backward. In forward decoding, the decoding starts with the first received block and proceeds forward to the last received block. In backward decoding the decoding starts with the last received block and proceeds backward. For illustration, in Fig. 4 node 3 decodes forward, while node 4 decodes backward. In both cases, the decoding uses the received signal received in two blocks, (74) together with

$$Y_3[i+1] = X_1(w_1[i+1]) + c_{32}X_2(w_2[i+1]) + c_{34}X_4[i+1] + Z_3[i+1]. \tag{75}$$

In forward decoding, the assumption is that $X_4[i]$ has been decoded successfully. The decoding starts by decoding $X_4[i+1]$ and decompressing it using Wyner–Ziv. This cooperation data is then used together with $Y_3'[i] = Y_3[i] - c_{34}X_4[i]$ to decode $X_1(w_1[i])$ (and possibly $X_2(w_2[i])$).

In backward decoding, the assumption is that $X_1(w_1[i+1])$ and $X_2(w_2[i+1])$ have been decoded successfully. As before,

TABLE I
ACHIEVABLE RATES FOR COMPRESS–FORWARD. THE RATE CONSTRAINTS ARE SHOWN FOR NODE 3, WITH A SYMMETRIC SET OF RATE CONSTRAINTS FOR NODE 4, GIVING A TOTAL OF NINE COMBINATIONS

Cooperation last	$\sigma_w^2 = \frac{\lvert c_{41}^2\rvert P_1+P_2+1+P_1+\lvert c_{32}\rvert^2P_2+\left(\lvert c_{32}\rvert^2\lvert c_{41}\rvert^2-2\mathrm{Re}\{c_{41}c_{32}\}+1\right)P_1P_2}{\lvert c_{34}\rvert^2P_4}$
- Individual decoding	$R_1 \le \log\left(1+\frac{\left(\lvert c_{41}\rvert^2+1+\sigma_w^2\right)P_1+\left(\lvert c_{32}\rvert^2\lvert c_{41}\rvert^2-2\mathrm{Re}\{c_{41}c_{32}\}+1\right)P_1P_2}{\left(\lvert c_{32}\rvert^2+\lvert c_{32}\rvert^2\sigma_w^2+1\right)P_2+1+\sigma_w^2}\right)$
- Joint decoding	$R_1 \le \log\left(1+P_1+\frac{\lvert c_{41}\rvert^2P_1}{1+\sigma_w^2}\right)$ $R_2 \le \log\left(1+\lvert c_{32}\rvert^2P_2+\frac{P_2}{1+\sigma_w^2}\right)$ $R_1+R_2 \le \log\left(1+P_1+\frac{\lvert c_{41}\rvert^2P_1}{1+\sigma_w^2}+\lvert c_{32}\rvert^2P_2+\frac{P_2}{1+\sigma_w^2}+\frac{\left(\lvert c_{32}\rvert^2\lvert c_{41}\rvert^2-2\mathrm{Re}\{c_{41}c_{32}\}+1\right)P_1P_2}{1+\sigma_w^2}\right)$
Cooperation first	$\sigma_w^2 = \frac{\lvert c_{41}\rvert^2(1+\lvert c_{34}\rvert^2P_4)P_1+(1+\lvert c_{34}\rvert^2P_4)P_2+1+\lvert c_{34}\rvert^2P_4+P_1+\lvert c_{32}\rvert^2P_2}{\lvert c_{43}\rvert^2P_3\left(P_1+\lvert c_{32}\rvert^2P_2+\lvert c_{34}\rvert^2P_4+1\right)}$ $+\frac{\left(\lvert c_{32}\rvert^2\lvert c_{41}\rvert^2-2\mathrm{Re}\{c_{41}c_{32}\}+1\right)P_1P_2}{\lvert c_{43}\rvert^2P_3\left(P_1+\lvert c_{32}\rvert^2P_2+\lvert c_{34}\rvert^2P_4+1\right)}$
- Joint decoding	$R_1 \le \log\left(1+\frac{P_1}{1+\lvert c_{34}\rvert^2P_4}+\frac{\lvert c_{41}\rvert^2P_1}{1+\sigma_w^2}\right)$ $R_2 \le \log\left(1+\frac{\lvert c_{32}\rvert^2P_2}{1+\lvert c_{34}\rvert^2P_4}+\frac{P_2}{1+\sigma_w^2}\right)$ $R_1+R_2 \le \log\left(1+\frac{P_1}{1+\lvert c_{34}\rvert^2P_4}+\frac{\lvert c_{41}\rvert^2P_1}{1+\sigma_w^2}+\frac{\lvert c_{32}\rvert^2P_2}{1+\lvert c_{34}\rvert^2P_4}+\frac{P_2}{1+\sigma_w^2}\right.$ $\left.+\frac{\left(\lvert c_{32}\rvert^2\lvert c_{41}\rvert^2-2\mathrm{Re}\{c_{41}c_{32}\}+1\right)P_1P_2}{\left(1+\sigma_w^2\right)\left(1+\lvert c_{34}\rvert^2P_4\right)}\right)$

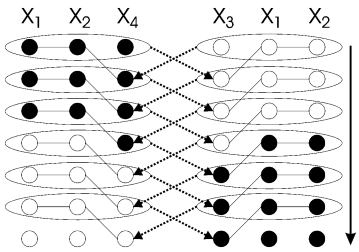

Fig. 4. Compress–forward coding. Arrows indicate forwarding, while solid lines indicate signals decoded jointly. Shaded circles indicate past decoded data. Node 3 (on the left) use forward decoding, while node 4 use backward decoding.

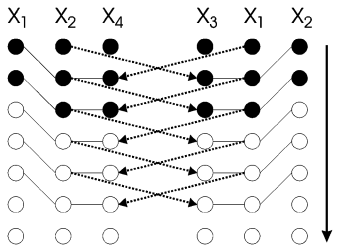

Fig. 5. Decode–forward with cooperation first. Arrows indicate forwarding, while solid lines indicate signals decoded jointly. Shaded circles indicate past decoded data.

the decoding starts by decoding $X_4[i+1]$ and decompressing is using Wyner–Ziv. This cooperation data is then used together with $Y_3[i]$ to decode $X_1(w_1[i])$ $X_2(w_2[i])$.

The difference between forward and backward decoding is that in forward decoding when $X_4[i+1]$ is (channel) decoded, $X_1(w_1[i+1])+c_{32}X_2(w_2[i+1])$ act as interference, but in backward decoding $X_4[i+1]$ is not subject to interference. On the other hand, in backward decoding $X_1(w_1[i])$ and $X_2(w_2[i])$ are subject to the interference from $X_4[i]$, while in forward decoding $X_1(w_1[i])$ and $X_2(w_2[i])$ are not subject to further interference. We therefore say that backward decoding uses *cooperation first* decoding, while forward decoding uses *cooperation last* decoding. Cooperation last and cooperation first give different rates, but which one is better depends on the channel state. Notice that this is specific to the multisource channel. In the relay channel, it is also possible to use either cooperation first and cooperation last decoding, but both for compress–forward and decode–forward it gives exactly the same rate.[3]

The resulting rates for cooperation are listed in Table I, with calculation of the rates in Appendix A.

[3]We explored that in connection with writing the paper [24], but this is not included in the final version of that paper exactly because it gives the same rate

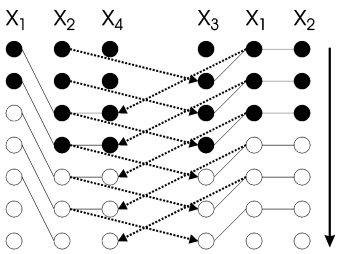

Fig. 6. Decode–forward with cooperation last for node 4. Arrows indicate forwarding, while solid lines indicate signal decoded jointly. Shaded circles indicate past decoded data.

2) Decode–Forward Coding: In decode–forward decoding, node 3 decodes the message w_2, re-encodes this as X_3, and forwards it to node 4, and node 4 decodes message w_1, re-encodes it as X_4, and forwards it to node 3. Thus, in general, a node has to jointly decode both messages w_1 and w_2, and because it has to forward the decoded message, decoding has to be forward. Still, the system can use *cooperation first* or *cooperation last* as in the compress–forward case, illustrated in Figs. 5 and 6.

TABLE II
ACHIEVABLE RATES FOR DECODE–FORWARD. THE LAST TWO ROWS ALSO HAVE MIRROR-SYMMETRIC SOLUTIONS WITH THE ROLE OF THE TWO RECEIVER NODES SWITCHED, FOR A TOTAL OF FIVE COMBINATIONS

	Node 3	Node 4
Cooperation first/ Cooperation first	$R_1 \le \log\left(1+P_1+\lvert c_{34}\rvert^2 P_4\right)$ $R_2 \le \log\left(1+\frac{\lvert c_{32}\rvert^2 P_2}{1+P_1}\right)$ $R_1+R_2 \le \log\left(1+P_1+\lvert c_{32}\rvert^2 P_2+\lvert c_{34}\rvert^2 P_4\right)$	$R_1 \le \log\left(1+\frac{\lvert c_{41}\rvert^2 P_1}{1+P_2}\right)$ $R_2 \le \log\left(1+P_2+\lvert c_{43}\rvert^2 P_3\right)$ $R_1+R_2 \le \log\left(1+\lvert c_{41}\rvert^2 P_1+P_2+\lvert c_{43}\rvert^2 P_3\right)$
Individual decoding	$R_1 \le \log\left(1+\frac{P_1+\lvert c_{34}\rvert^2 P_4}{1+\lvert c_{32}\rvert^2 P_2}\right)$	$R_1 \le \log\left(1+\lvert c_{41}\rvert^2 P_1\right)$ $R_2 \le \log\left(1+P_2\right)$ $R_1+R_2 \le \log\left(1+\lvert c_{41}\rvert^2 P_1+P_2\right)$
Cooperation first/ Cooperation last	$R_1 \le \log\left(1+P_1+\lvert c_{34}\rvert^2 P_4\right)$ $R_2 \le \log\left(1+\frac{\lvert c_{32}\rvert^2 P_2}{1+P_1}\right)$ $R_1+R_2 \le \log\left(1+P_1+\lvert c_{32}\rvert^2 P_2+\lvert c_{34}\rvert^2 P_4\right)$	$R_1 \le \log\left(1+\lvert c_{41}\rvert^2 P_1\right)$ $R_2 \le \log\left(1+P_2\right)+\log\left(1+\frac{\lvert c_{43}\rvert^2 P_3}{1+\lvert c_{41}\rvert^2 P_1+P_2}\right)$ $R_1+R_2 \le \log\left(1+\lvert c_{41}\rvert^2 P_1+P_2+\lvert c_{43}\rvert^2 P_3\right)$

In Fig. 5, both nodes use cooperation first in a symmetric way. Consider node 4 with a received signal

$$\begin{aligned} Y_4[i-1] &= c_{41}X_1(w_1[i-1]) + X_2(w_2[i-1]) \\ &\quad + c_{43}X_3(w_2[i-2]) + Z_4[i] \qquad (76) \\ Y_4[i] &= c_{41}X_1(w_1[i]) + X_2(w_2[i]) \\ &\quad + c_{43}X_3(w_2[i-1]) + Z_4[i]. \qquad (77) \end{aligned}$$

At time i, node 4 decodes $w_1[i]$ and $w_2[i-1]$ jointly using $X_1(w_1[i])$, $X_2(w_2[i-1])$, and $X_3(w_2[i-1])$. Notice that X_1 does not interfere when X_3 is used.

In Fig. 6, node 4 uses cooperation last. The received signal is the same, but at time i node 4 now decodes $w_1[i-1]$ and $w_2[i-1]$ jointly using the $X_1(w_1[i-1])$, $X_2(w_2[i-1])$, and $X_3(w_2[i-1])$. Notice that in this case, X_1 does interfere when X_3 is used, which is is the difference from cooperation first. In Fig. 6, node 3 still does cooperation first decoding but with a larger delay. It can be seen that at least one node has to do cooperation first, as opposed to the case of compress–forward.

Table II summarizes the achievable rates, with the rate calculations in Appendix A. For individual decoding, node 3 only decodes its own message and does not help node 4, while node 4 decodes both messages and forwards message w_1 to node 3 to help.

3) High-SNR Offset: The expressions for compress–forward look complicated for finite SNR. However, taking the limit $\sigma^2 \to 0$ is a straightforward exercise, which result in the following proposition

Proposition 4: "Compress–forward with cooperation last and joint decoding" gives a high-SNR offset of

$$a = \min\Big\{\log\left(\lvert c_{41}\rvert^2 P_1 + P_2 + \lvert c_{43}\rvert^2 P_3\right), \log\left(P_1 + \lvert c_{32}\rvert^2 P_2 + \lvert c_{34}\rvert^2 P_4\right)\Big\}. \qquad (78)$$

All other cooperation schemes give a high-SNR offset which is at most equal to the offset (27) without cooperation.

For $\lvert c_{32}\rvert, \lvert c_{41}\rvert > 1$, (78) equals the upper bound (72) except for the $\log\left(1+\lvert c_{41}\rvert^{-2}\right)$ term. This it at most a 3-dB gap, and for $\lvert c_{32}\rvert, \lvert c_{41}\rvert \gg 1$ much smaller. We can therefore say that compress–forward acheives capacity asymptotically as $\sigma^2 \to 0$ and $\lvert c_{32}\rvert, \lvert c_{41}\rvert \to \infty$. Furthermore, compared to no cooperation (27), the terms $\lvert c_{43}\rvert^2 P_3$ and $\lvert c_{34}\rvert^2 P_4$ essentially characterize the gain from receiver cooperation in the high-SNR regime, at least for $\lvert c_{32}\rvert, \lvert c_{41}\rvert > 1$.

For $\lvert c_{32}\rvert, \lvert c_{41}\rvert < 1$, there can be a large gap between the upper bound and the achievable rate, and we do not know at present how to close this gap.

The fact that all other cooperation scheme gives no gain in the high-SNR regime does does not mean they are without interest, as they can be superior in the medium-SNR regime. For example, numerical experiments (which we have not included) show that "Compress–forward with cooperation last" generally has poor performance in the low-to-medium SNR regime, whereas "Compress–forward with cooperation first" has a performance close to the upper bound in this region.

4) The Synchronous Case: The difference between the upper bounds for the asynchronous and synchronous case is the last term, $2\sqrt{\lvert c_{43}\rvert^2 P_2 P_3 + \lvert c_{41}\rvert^2 \lvert c_{43}\rvert^2 P_1 P_3}$, inside the log (47). This term is less than or equal to the first term inside the log. Thus, comparing upper bounds, the gain from synchronization is at most 3 dB (in the numerical examples later in the paper, Figs. 10 and 11, the gap is no more than a fraction of a decibel). At the same time, Proposition 4 shows that at least for strong interference in the high-SNR regime, the achievable rate in the asynchronous case comes within 3 dB of the upper bound. This indicates, although not a proof, that the gain from synchronization for receiver cooperation is very limited, at most a few decibels. Additionally, it is not clear how to extend compress–forward to take advantage of synchronization. For this reason, it seems it does not pay to do synchronization for receiver cooperation, and we will not consider this further.

VI. TRANSMITTER COOPERATION

In transmitter cooperation, the two source nodes: 1 and 2, cooperate on transmitting the signal by "eavesdropping" on the communication signals, see Fig. 1(b). Notice that, as already mentioned, no new energy is introduced into the system, as opposed to receiver cooperation. We will first derive outer bounds for the capacity region, and then a number of different coding methods.

A. Outer Bound

The max-flow-min-cut theorem [23, Theorem 14.10.1] gives the following bounds:

$$R_1 \le I(x_1; y_2, y_3|x_2) \tag{79}$$
$$R_2 \le I(x_2; y_1, y_4|x_1) \tag{80}$$
$$R_1 \le I(x_1, x_2; y_3) \tag{81}$$
$$R_2 \le I(x_1, x_2; y_4) \tag{82}$$
$$R_1 + R_2 \le I(x_1, x_2; y_3, y_4) \tag{83}$$

where the y_i are governed by the system model (12). If we let $E[x_1 x_2^*] = \alpha\sqrt{P_1 P_2}$ then

$$\mathrm{var}(x_1|x_2) = (1 - |\alpha|^2)P_1 \tag{84}$$
$$\mathrm{var}(x_2|x_1) = (1 - |\alpha|^2)P_2 \tag{85}$$
$$\mathrm{var}(ax_1 + bx_2) = |a|^2 P_1 + |b|^2 P_2 + 2\mathrm{Re}\{\alpha a b^*\}\sqrt{P_1 P_2}. \tag{86}$$

We then get the following bounds:

$$R_1 \le \log\left(1 + (1 - |\alpha|^2)P_1\left(|c_{21}|^2 + 1\right)\right) \tag{87}$$
$$R_2 \le \log\left(1 + (1 - |\alpha|^2)P_2\left(|c_{12}|^2 + 1\right)\right) \tag{88}$$
$$R_1 \le \log\left(1 + P_1 + |c_{32}|^2 P_2 + 2\mathrm{Re}\{\alpha c_{32}\}\sqrt{P_1 P_2}\right) \tag{89}$$
$$R_2 \le \log\left(1 + P_2 + |c_{41}|^2 P_1 + 2\mathrm{Re}\{\alpha^* c_{41}\}\sqrt{P_1 P_2}\right) \tag{90}$$
$$R_1 + R_2 \le \log\Bigg(1 + (1 + |c_{32}|^2)P_2 + (1 + |c_{41}|^2)P_1 + \left|c_{32}c_{41}^* - 1\right|^2\left(1 - |\alpha|^2\right)P_1 P_2 + 2\mathrm{Re}\left\{c_{32}\alpha + c_{41}^*\alpha^*\right\}\sqrt{P_1 P_2}\Bigg). \tag{91}$$

The bound on the sum rate can be strengthened by the same argument used to find the upper bound in [35]: the capacity region only depends on the *marginal* noise distribution at nodes 3 and 4, and is therefore not changed if the noise at nodes 3 and 4 are made correlated. We can then bound the sum rate as follows:

$$R_1 + R_2 \le \min_{\boldsymbol{\Sigma}_z} \log\left(\frac{\left|\boldsymbol{H}\boldsymbol{\Sigma}_x\boldsymbol{H}^H + \boldsymbol{\Sigma}_z\right|}{|\boldsymbol{\Sigma}_z|}\right) \tag{92}$$

where $\boldsymbol{\Sigma}_z$ is the covariance matrix of the noise, given by

$$\boldsymbol{\Sigma}_z = \begin{bmatrix} 1 & re^{i\theta} \\ re^{-i\theta} & 1 \end{bmatrix} \tag{93}$$

and $\boldsymbol{\Sigma}_x$ is the covariance matrix of the transmitted signals, which depends on α. The minimum in (92) can be found explicitly. Define

$$\boldsymbol{K} = \boldsymbol{H}\boldsymbol{\Sigma}_x\boldsymbol{H}^H. \tag{94}$$

Then

$$|\boldsymbol{K}+\Sigma_z| = \begin{vmatrix} k_{11}+1 & k_{12}+re^{i\theta} \\ k_{12}^*+re^{-i\theta} & k_{22}+1 \end{vmatrix} \tag{95}$$
$$= (k_{11}+1)(k_{22}+1) - |k_{12}|^2 - 2r\mathrm{Re}\{k_{12}e^{-i\theta}\} - r^2 \tag{96}$$
$$= (k_{11}+1)(k_{22}+1) - |k_{12}|^2 - 2r|k_{12}| - r^2 \tag{97}$$
$$\frac{|\boldsymbol{K}+\Sigma_z|)}{|\boldsymbol{\Sigma}_z|} = \frac{(k_{11}+1)(k_{22}+1) - |k_{12}|^2 - 2r|k_{12}| - r^2}{1 - r^2} \tag{98}$$

where the equalities (96) and (97) are by choosing the optimum phase: $e^{i\theta} = \angle k_{12}$. Let $C = (k_{11}+1)(k_{22}+1) - |k_{12}|^2$. Then the optimum choice of r is found by differentiation to be

$$r = \frac{(C-1) - \sqrt{(C-1)^2 - 4|k_{12}|^2}}{2|k_{12}|}. \tag{99}$$

Bounds for the asynchronous case is found by simply putting $\alpha = 0$ in the above bounds (cf. Lemma 1 in [24]). As for receiver cooperation, we have the following additional bound that considerably tightens the upper bound.

Theorem 2: Consider transmitter cooperation. If $|c_{41}| < 1$, the following bound applies in the asynchronous case:

$$R_2 \le \log\left(\frac{1 + |c_{41}|^2 P_1 + P_2}{|c_{41}|^2 2^{R_1}\frac{1+P_1}{1+(1+|c_{21}|^2)P_1} + 1 - |c_{41}|^2}\right) \tag{100}$$

and in the synchronous case

$$R_2 \le \log\left(\frac{1 + \left(|c_{41}|\sqrt{P_1} + \sqrt{P_2}\right)^2}{|c_{41}|^2 2^{R_1}\frac{1+P_1}{1+(1+|c_{21}|^2)P_1} + 1 - |c_{41}|^2}\right). \tag{101}$$

Furthermore, the resulting bound on $R_1 + R_2$ is an increasing function of R_1.

If $|c_{41}| > 1$, the following bound applies in the asynchronous case:

$$R_1 + R_2 \le \log\left(1 + |c_{41}|^2 P_1 + P_2\right) + \log\left(\frac{1 + \left(|c_{41}|^2 + |c_{21}|^2\right)P_1}{1 + |c_{41}|^2 P_1}\right) \tag{102}$$

and in the synchronous case

$$R_1 + R_2 \le \log\left(1 + \left(|c_{41}|\sqrt{P_1} + \sqrt{P_2}\right)^2\right) + \log\left(\frac{1 + \left(|c_{41}|^2 + |c_{21}|^2\right)P_1}{1 + |c_{41}|^2 P_1}\right). \tag{103}$$

Proof: We first assume $|c_{41}| \le 1$. We transform the system as in indicated in Fig. 7 to a system with equal or larger capacity region. The argument for the step of Fig. 7(a) to Fig. 7(b) is as follows: Node 3 is given the received signal at node 2 as side information, i.e., $y_3'[i] = c_{21}x_1[i] + z_2[i]$, as well as the message w_2. Node 1 is given as side information $y_3'[i]$

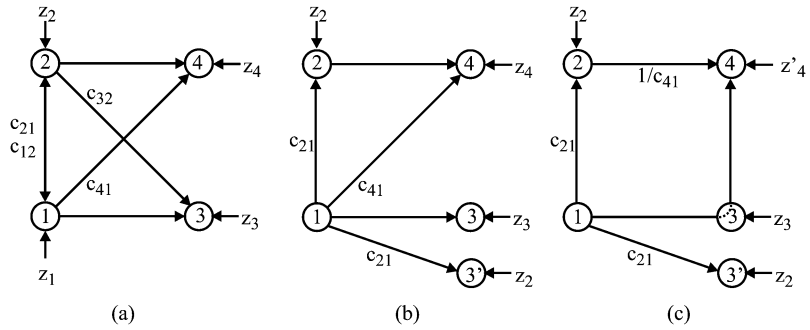

Fig. 7. Channel transformations used in the proof of Theorem 2. All noise variables z_i are independent, and all have power 1, except z_4' which has power $\frac{1-|c_{41}|^2}{|c_{41}|^2}$.

and w_2. The link between nodes 2 and 3 can now be deleted, as node 3, with knowledge of w_2 and the received signal $y_3'[i]$ knows what node 2 transmits. Similarly, the link from node 2 to node 1 can be deleted. In the step of Fig. 7(b) to Fig. 7(c), we replace $y_4[i]$ with a degraded version of $y_3[i]$

$$\begin{aligned} y_4[i] &= y_3[i] + c_{41}^{-1}x_2[i] + z_4'[i] \\ &= x_1[i] + c_{41}^{-1}x_2[i] + z_3[i] + z_4'[i] \end{aligned} \tag{104}$$

where

$$E\left[|z_4'[i]|^2\right] = \frac{1-|c_{41}|^2}{|c_{41}|^2}. \tag{105}$$

This can be done because $y_4[i]$ in Fig. 7(b) and in Fig. 7(c) have the same marginal distributions (except for a scaling). The capacity regions for the two systems are therefore identical since they only depend on the marginal distribution of the received signals at the destinations as they do not cooperate.

First, we can bound R_1 as follows using the chain rule:

$$\begin{aligned} nR_1 &\le H(\boldsymbol{y}_3[n], \boldsymbol{y}_3'[n]|w_2) - H(\boldsymbol{y}_3[n], \boldsymbol{y}_3'[n]|\boldsymbol{x}_1[n], w_2) \\ &\quad + n\epsilon_n \qquad (106) \\ &= \sum_{i=1}^{n} H\left(y_3[i], y_3'[i]|\boldsymbol{y}_3[i-1], \boldsymbol{y}_3'[i-1], w_2\right) \\ &\quad - \sum_{i=1}^{n} \left(H(z_3[i]) + H(z_2[i])\right) + n\epsilon_n \qquad (107) \\ &= \sum_{i=1}^{n} H\left(y_3'[i]|y_3[i], \boldsymbol{y}_3[i-1], \boldsymbol{y}_3'[i-1], w_2\right) \\ &\quad + \sum_{i=1}^{n} H\left(y_3[i]|\boldsymbol{y}_3[i-1], \boldsymbol{y}_3'[i-1], w_2\right) \\ &\quad - \sum_{i=1}^{n} \left(H(z_3[i]) + H(z_2[i])\right) + n\epsilon_n \qquad (108) \\ &\le \sum_{i=1}^{n} H\left(y_3'[i]|y_3[i]\right) \\ &\quad + \sum_{i=1}^{n} H\left(y_3[i]|\boldsymbol{y}_3[i-1], \boldsymbol{y}_3'[i-1], w_2\right) \\ &\quad - \sum_{i=1}^{n} \left(H(z_3[i]) + H(z_2[i])\right) + n\epsilon_n. \qquad (109) \end{aligned}$$

Here

$$\begin{aligned} H\left(y_3'[i]|y_3[i]\right) &\le \log(2\pi e) + \log E\left[\mathrm{var}[y_3'[i]|y_3[i]]\right] \qquad (110) \\ &= \log(2\pi e) + \log\Big(E\left[\mathrm{var}[c_{21}x_1[i]|x_1[i] + z_3[i]\right] \\ &\quad + \mathrm{var}[z_2[i]]\Big). \qquad (111) \end{aligned}$$

By Lemma 1

$$\begin{aligned} E\left[\mathrm{var}[c_{21}x_1[i]|x_1[i] + z_3[i]]\right] &\le |c_{21}|^2 P_1 - \frac{(|c_{21}|P_1)^2}{P_1 + 1} \qquad (112) \\ &= \frac{|c_{21}|^2 P_1}{1 + P_1}. \qquad (113) \end{aligned}$$

Then

$$\begin{aligned} &\sum_{i=1}^{n} H\left(y_3[i]|\boldsymbol{y}_3[i-1], \boldsymbol{y}_3'[i-1], w_2\right) \\ &\quad \ge nR_1 + n\log\left(2\pi e \frac{1+P_1}{1+(1+|c_{21}|^2)P_1}\right) - n\epsilon_n. \qquad (114) \end{aligned}$$

The rate R_2 can be bounded by

$$nR_2 \le H(\boldsymbol{y}_4[n]) - H(\boldsymbol{y}_4[n]|w_2) + n\epsilon_n. \tag{115}$$

The entropy $H(\boldsymbol{y}_4[n])$ is bounded by

$$\begin{aligned} H(\boldsymbol{y}_4[n]) &\le n\log(2\pi e) \\ &\quad + n\log\left(1 + P_1 + \frac{1-|c_{41}|^2}{|c_{41}|^2} + \frac{P_2}{|c_{41}|^2}\right) \end{aligned} \tag{116}$$

in the asynchronous case, and

$$\begin{aligned} H(\boldsymbol{y}_4[n]) &\le n\log(2\pi e) \\ &\quad + n\log\Bigg(1 + P_1 + \frac{1-|c_{41}|^2}{|c_{41}|^2} \\ &\quad + \frac{P_2 + 2|c_{41}|\sqrt{P_1P_2}}{|c_{41}|^2}\Bigg) \end{aligned} \tag{117}$$

in the synchronous case.

$$H(\boldsymbol{y}_4[n]|w_2) = \sum_{i=1}^{n} H(y_4[i]|\boldsymbol{y}_4[i-1], w_2) \tag{118}$$

$$\geq \sum_{i=1}^{n} H\left(y_3[i] + c_{41}^{-1}x_2[i] + z_4'[i]|\boldsymbol{y}_4[i-1], w_2, \boldsymbol{x}_2[i]\right) \tag{119}$$

$$= \sum_{i=1}^{n} H\left(y_3[i] + z_4'[i]|\boldsymbol{y}_4[i-1], w_2, \boldsymbol{x}_2[i]\right) \tag{120}$$

$$\geq \sum_{i=1}^{n} H\left(y_3[i] + z_4'[i]|\boldsymbol{y}_4[i-1], w_2, \boldsymbol{x}_2[i], \boldsymbol{y}_3[i-1], \boldsymbol{y}_3'[i-1]\right) \tag{121}$$

$$= \sum_{i=1}^{n} H\left(y_3[i] + z_4'[i]|w_2, \boldsymbol{y}_3[i-1], \boldsymbol{y}_3'[i-1]\right) \tag{122}$$

The entropy $H(\boldsymbol{Y}_4[n]|w_2)$ can by lower-bounded as shown in (118)–(122) at the top of the page, where we have repeatedly used that conditioning reduces entropy. In (121) and (122), we have used that $\boldsymbol{y}_4[i-1] = \boldsymbol{y}_3[i-1] + c_{41}^{-1}\boldsymbol{x}_2[i-1]$ and that $\boldsymbol{x}_2[i]$ depends only on w_2 and $\boldsymbol{y}_3'[i-1]$.

We can now use the (conditional) entropy power inequality [51], [37, Theorem 16.6.3] (the conditional version follows as in [52])

$$H\left(y_3[i] + z_4'[i]|w_2, \boldsymbol{y}_3[i-1], \boldsymbol{y}_3'[i-1]\right) \geq \log\left(2^{H\left(y_3[i]|w_2, \boldsymbol{y}_3[i-1], \boldsymbol{y}_3'[i-1]\right)} + 2\pi e \mathrm{var}\left[z_4'[i]\right]\right). \tag{123}$$

Then we get (124)–(126) at the bottom of the page, where the last inequality is due to Jensen's inequality [37, Theorem 2.6.1]. Inserting (114) into this, using (116), and letting $n \to \infty$, we finally get

$$R_2 \leq \log\left(\frac{1 + |c_{41}|^2 P_1 + P_2}{|c_{41}|^2 2^{R_1 \frac{1+P_1}{1+(1+|c_{21}|^2)P_1}} + 1 - |c_{41}|^2}\right) \tag{127}$$

in the asynchronous case. The synchronous case follows similarly by using (117). It can be seen, for example by differentiation, that the sum $R_1 + R_2$ is an increasing function of R_1.

For $|c_{41}| > 1$, the above proof is still valid, except the step from Fig.7 (b) to (c), as (105) becomes negative. This is solved by increasing the gain in on the link between nodes 1 and 3 from 1 to $|c_{41}|$ in Fig. 7(b), which can only enlarge the capacity region. Equivalently, to stay with the normalized channel model, this can be accomplished by increasing the power P_1 to $|c_{41}|^2 P_1$ in Fig. 7(b) and dividing c_{21} with $|c_{41}|$. The above proof for $|c_{41}| \leq 1$ now applies (with $z_4'[i] = 0$), and the bound (127) is valid with $|c_{41}| = 1$, P_1 replaced with $|c_{41}|^2 P_1$, and $|c_{21}|^2$ replaced with $\frac{|c_{21}|^2}{|c_{41}|^2}$, which gives

$$R_2 \leq \log\left(\frac{1 + |c_{41}|^2 P_1 + P_2 + |c_{43}|^2 P_3}{2^{R_1 \frac{1+|c_{41}|^2 P_1}{1+(|c_{21}|^2+|c_{41}|^2)P_1}}}\right). \tag{128}$$

The bound (102) on $R_1 + R_2$ is directly obtained from this, and similarly for (103). □

By similar arguments as used for Proposition 2 we get the following results for the high-SNR regime.

Proposition 5: The multiplexing factor from transmitter cooperation is $m = 1$. If $|c_{41}| < 1$ the high-SNR offset in the asynchronous case is bounded by

$$a \leq \log\left(|c_{41}|^2 P_1 + P_2\right) + \log\left(\frac{1 + |c_{21}|^2}{|c_{41}|^2}\right) \tag{129}$$

and in the synchronous case by

$$a \leq \log\left(\left(|c_{41}|\sqrt{P_1} + \sqrt{P_2}\right)^2\right) + \log\left(\frac{1 + |c_{21}|^2}{|c_{41}|^2}\right). \tag{130}$$

If $|c_{41}| > 1$, the high-SNR offset in the asynchronous case is bounded by

$$a \leq \log\left(|c_{41}|^2 P_1 + P_2\right) + \log\left(1 + \frac{|c_{21}|^2}{|c_{41}|^2}\right) \tag{131}$$

and in the synchronous case by

$$a \leq \log\left(\left(|c_{41}|\sqrt{P_1} + \sqrt{P_2}\right)^2\right) + \log\left(1 + \frac{|c_{21}|^2}{|c_{41}|^2}\right). \tag{132}$$

$$H(\boldsymbol{y}_4|w_2) \geq n \sum_{i=1}^{n} \frac{1}{n} H\left(y_3[i] + z_4'[i]|w_2, \boldsymbol{y}_3[i-1], \boldsymbol{y}_3'[i-1]\right) + n \log|c_{41}|^2 \tag{124}$$

$$\geq n \sum_{i=1}^{n} \frac{1}{n} \log\left(2^{H\left(y_3[i]|w_2, \boldsymbol{y}_3[i-1], \boldsymbol{y}_3'[i-1]\right)} + 2\pi e \mathrm{var}\left[z_4'[i]\right]\right) + n \log|c_{41}|^2 \tag{125}$$

$$\geq n \log\left(2^{\sum_{i=1}^{n} \frac{1}{n} H\left(y_3[i]|w_2, \boldsymbol{y}_3[i-1], \boldsymbol{y}_3'[i-1]\right)} + 2\pi e \mathrm{var}\left[z_4'[i]\right]\right) + n \log|c_{41}|^2 \tag{126}$$

TABLE III
ACHIEVABLE RATES FOR TRANSMITTER COOPERATION IN THE ASYNCHRONOUS CASE. THE BOUNDS CAN BE OPTIMIZED WITH RESPECT TO A_1, $\tilde{A}_1$, A_2, AND $\tilde{A}_2$ SUBJECT TO $A_1^2+\tilde{A}_1^2 \le P_1$ AND $A_2^2+\tilde{A}_2^2 \le P_2$. IN ADDITION TO THE CASES LISTED IN THE TABLE THERE ARE THE MIRROR-SYMMETRIC CASES WHERE THE TWO SOURCE–DESTINATION PAIRS ARE EXCHANGED, AND THE CASE OF NO COOPERATION, FOR A TOTAL OF 13 CASES

Node 1	Node 2	Node 3	Node 4
forwarding $R_2 \le \log(1+\lvert c_{12}\rvert^2 P_2)$	forwarding $R_1 \le \log(1+\lvert c_{21}\rvert^2 P_1)$	joint $R_1+R_2 \le \log(1+P_1+\lvert c_{32}\rvert^2 P_2)$	joint $R_1+R_2 \le \log(1+\lvert c_{41}\rvert^2 P_1+P_2)$
	forwarding $R_1 \le \log(1+\lvert c_{21}\rvert^2 P_1)$	joint $R_2 \le \log(1+\lvert c_{32}\rvert^2 P_2)$ $R_1+R_2 \le \log(1+P_1+\lvert c_{32}\rvert^2 P_2)$	joint $R_2 \le \log(1+P_2)$ $R_1+R_2 \le \log(1+\lvert c_{41}\rvert^2 P_1+P_2)$
forwarding $R_2 \le \log(1+\lvert c_{12}\rvert^2 A_2^2)$	forwarding $R_1 \le \log(1+\lvert c_{21}\rvert^2 A_1^2)$	individual $R_1 \le \log\left(1+\frac{A_1^2+\lvert c_{32}\rvert^2\tilde{A}_2^2}{1+\tilde{A}_1^2+\lvert c_{32}\rvert^2 A_2^2}\right)$	individual $R_2 \le \log\left(1+\frac{A_2^2+\lvert c_{41}\rvert^2\tilde{A}_1^2}{1+\tilde{A}_2^2+\lvert c_{41}\rvert^2 A_1^2}\right)$
	forwarding $R_1 \le \log(1+\lvert c_{21}\rvert^2 P_1)$	individual $R_1 \le \log\left(1+\frac{P_1+\lvert c_{32}\rvert^2\tilde{A}_2^2}{1+\lvert c_{32}\rvert^2 A_2^2}\right)$	individual $R_2 \le \log\left(1+\frac{A_2^2}{1+\lvert c_{41}\rvert^2 P_1}\right)$
forwarding $R_2 \le \log(1+\lvert c_{12}\rvert^2 A_2^2)$	forwarding $R_1 \le \log(1+\lvert c_{21}\rvert^2 A_1^2)$	joint $R_1 \le \log\left(1+A_1^2+\lvert c_{32}\rvert^2\tilde{A}_2^2\right)$ $R_1+R_2 \le \log(1+P_1+\lvert c_{32}\rvert^2 P_2)$	individual $R_2 \le \log\left(1+\frac{A_2^2+\lvert c_{41}\rvert^2\tilde{A}_1^2}{1+\tilde{A}_2^2+\lvert c_{41}\rvert^2 A_1^2}\right)$
	forwarding $R_1 \le \log(1+\lvert c_{21}\rvert^2 P_1)$	joint $R_1 \le \log\left(1+P_1+\lvert c_{32}\rvert^2\tilde{A}_2^2\right)$ $R_1+R_2 \le \log(1+P_1+\lvert c_{32}\rvert^2 P_2)$	individual $R_2 \le \log\left(1+\frac{A_2^2}{1+\tilde{A}_2^2+\lvert c_{41}\rvert^2 P_1}\right)$
forwarding $R_2 \le \log(1+\lvert c_{12}\rvert^2 P_2)$		joint $R_1 \le \log\left(1+A_1^2\right)$ $R_1+R_2 \le \log(1+P_1+\lvert c_{32}\rvert^2 P_2)$	individual $R_2 \le \log\left(1+\frac{P_2+\lvert c_{41}\rvert^2\tilde{A}_1^2}{1+\lvert c_{41}\rvert^2 A_1^2}\right)$

B. Achievable Rate in the Asynchronous Case

We will limit our consideration to decode–forward coding. Each transmitter decodes the other transmitter's message stream and forwards the messages. For this to be possible, a transmitter must be able to decode the other transmitter's messages, and that puts a basic constraint on the rates, no matter how the encoding is done

$$R_1 \le \log(1+|c_{21}|^2 P_1) \tag{133}$$
$$R_2 \le \log(1+|c_{12}|^2 P_2). \tag{134}$$

However, it may pay off that only one node cooperates, while the other transmission is direct. In that case, only one of the bounds (133) and (134) apply.

The destination nodes use either joint decoding of the two messages, or individual decoding considering the undesired signal as part of the Gaussian noise. If a destination node, say node 3, is using joint decoding, the cooperating node, node 2 here, can also use joint encoding of the messages, multiplexed coding. Otherwise, node 2 uses superposition of its own information, dedicating a power A_2^2 for this, and the cooperation information, with power $\tilde{A}_2^2$. This gives a number of different possibilities that are outlined in Table III. The proof is in Appendix B.

It can be seen that none of the cooperation schemes give any gain over no cooperation in the high-SNR regime. On the other hand, Proposition 5 indicates that there might be a potential gain. To realize this we need to consider synchronous systems.

C. Achievable Rate in the Synchronous Case

The most significant gain that results from synchronized transmitters is the ability to null interference, combined with "dirty-paper" coding using the fact that signals are now completely known including phase. This was used in [35] for the multiple-antenna broadcast channel and is what gives the multiplexing gain in rate. Recently [45], this was proven to in fact give the total capacity region of the multiple-antenna broadcast channel. We will therefore concentrate on generalizing this to transmitter cooperation. This kind of coding method was first presented in [28].

We consider the case where both receivers use individual decoding, i.e., consider the undesired signal as interference. The transmission in block i is

$$\begin{bmatrix} X_1[i] \\ X_2[i] \end{bmatrix} = \begin{bmatrix} A_1 & 0 \\ 0 & A_2 \end{bmatrix} \begin{bmatrix} U_1\left(w_1[i], w_1[i-1], U_1^0, U_2^0\right) \\ U_2\left(w_2[i], U_1^0\right) \end{bmatrix} + \begin{bmatrix} t_{11} & t_{12} \\ t_{21} & t_{22} \end{bmatrix} \begin{bmatrix} U_1^0\left(w_1[i-1], U_2^0\right) \\ U_2^0(w_2[i-1]) \end{bmatrix} \tag{135}$$

where A_i are some real constants, and t_{ij} are some complex constants. All of the codes U_1, U_2, U_1^0, and U_2^0 are independent i.i.d. Gaussian codebooks of power 1. The code U_2^0 is a standard Gaussian code for $w_2[i-1]$. The code U_1^0 encodes $w_1[i-1]$ with "dirty-paper" coding using U_2^0 as interference (which at the time of coding is known at both sources). The code U_2 encodes $w_2[i]$ with "dirty-paper" coding using U_1^0 as interference. Finally, U_1 jointly encodes $w_1[i]$ and $w_1[i-1]$ using multiplexed coding combined with "dirty-paper" coding using a linear combination of U_1^0 and U_2^0 as interference.

Node 1 transmits U_1 alone with a power A_1^2 and node 2 alone transmits U_2 with a power A_2^2. Node 1 additionally transmits, using superposition, the linear combination $t_{11}U_1^0 + t_{12}U_2^0$. It can do so because U_1^0 and U_2^0 only depend on *past* codewords, which have been decoded under the decode–forward assumption. Similarly for node 2.

The power constraint for this transmission scheme is

$$A_1^2+|t_{11}|^2+|t_{12}|^2 \le P_1$$
$$A_2^2+|t_{21}|^2+|t_{22}|^2 \le P_2. \tag{136}$$

We will next derive the rate region achievable by this coding scheme for fixed A_i and t_{ij}.

First, nodes 1 and 2 must be able to decode each others' messages. Consider node 2, which has a received signal

$$\begin{aligned} Y_2[i] &= c_{21}A_1U_1\left(w_1[i], w_1[i-1], U_1^0, U_2^0\right) \\ &\quad + c_{21}\left(t_{11}U_1^0\left(w_1[i-1], U_2^0\right) + t_{12}U_2^0(w_2[i-1])\right) \\ &\quad + Z_2[i]. \end{aligned} \tag{137}$$

Node 2 knows U_1^0, and U_2^0 perfectly, so it can subtract them to form

$$Y_2'[i] = c_{21}A_1U_1\left(w_1[i], w_1[i-1], U_1^0, U_2^0\right) + Z_2[i]. \tag{138}$$

As node 2 knows $w_1[i-1]$ by the forward decoding assumption, and also U_1^0 and U_2^0, it can decode $w_1[i]$ if [4]

$$R_1 \le \log\left(1 + |c_{21}|^2A_1^2\right). \tag{139}$$

Similarly, node 1 can decode $w_2[i]$ if

$$R_2 \le \log\left(1 + |c_{12}|^2A_2^2\right). \tag{140}$$

Now consider decoding at node 4. Node 4 uses forward decoding, so by assumption at time i it has decoded $w_2[i-2]$. It then forms

$$\begin{aligned} Y_4'[i-1] &= Y_4[i-1] - (c_{41}t_{12} + t_{22})U_2^0(w_2[i-2]) \\ &= A_2U_2\left(w_2[i-1], U_1^0\right) \\ &\quad + (c_{41}t_{11} + t_{21})U_1^0\left(w_1[i-2], U_2^0\right) \\ &\quad + c_{41}A_1U_1\left(w_1[i-1], U_2^0\right) + Z_4[i-1] \end{aligned} \tag{141}$$

$$\begin{aligned} Y_4[i] &= A_2U_2\left(w_2[i], U_1^0\right) + (c_{41}t_{12} + t_{22})U_2^0(w_2[i-1]) \\ &\quad + (c_{41}t_{11} + t_{21})U_1^0\left(w_1[i-1], U_2^0\right) \\ &\quad + c_{41}A_1U_1\left(w_1[i], U_1^0, U_2^0\right) + Z_4[i+1]. \end{aligned} \tag{142}$$

The signals $(Y_4'[i-1], Y_4[i])$ form two channels in parallel for decoding of $w_2[i-1]$. In the first, U_2 has been "dirty-paper" coded with U_1^0 as "dirt," so that U_1^0 does not result in interference. In the second channel, U_2^0 is subject to all interference. Therefore, node 4 can decode $w_2[i-1]$ if

$$\begin{aligned} R_2 &\le \log\left(1 + \frac{A_2^2}{1 + |c_{41}|^2A_1^2}\right) \\ &\quad + \log\left(1 + \frac{|c_{41}t_{12} + t_{22}|^2}{1 + A_2^2 + |c_{41}t_{11} + t_{21}|^2 + |c_{41}|^2A_1^2}\right). \end{aligned} \tag{143}$$

Node 3 uses backward decoding, i.e., it uses the received signal

$$\begin{aligned} Y_3[i] &= A_1U_1\left(w_1[i], w_1[i-1], U_1^0, U_2^0\right) \\ &\quad + (t_{11} + c_{32}t_{21})U_1^0\left(w_1[i-1], U_2^0\right) \\ &\quad + (t_{12} + c_{32}t_{22})U_2^0(w_2[i-1]) \\ &\quad + c_{32}A_2U_2\left(w_2[i], U_1^0\right) + Z_3[i] \end{aligned} \tag{144}$$

assuming that $w_1[i]$ has been decoded. Notice that both codewords for $w_1[i-1]$ have been "dirty-paper" coded with knowledge of U_2^0, so that the rate constraint is

$$R_1 \le \log\left(1 + \frac{|t_{11} + c_{32}t_{21}|^2 + A_1^2}{1 + |c_{32}|^2A_2^2}\right). \tag{145}$$

This leaves an optimization problem over the real A_i and the complex t_{ij}. It does not seem possible to do this optimization analytically, and the numerical optimization problem is not convex and also seems very sensitive to small deviations from optimality. We will briefly discuss how the optimization complexity can be somewhat reduced. First, the optimal choice of phase for t_{12} and t_{22} is so that $c_{41}t_{12}$ and t_{22} have the same phase, so that in (143)

$$|c_{41}t_{12} + t_{22}|^2 = |t_{22}|^2 + |c_{41}|^2|t_{12}|^2 + 2|c_{41}||t_{22}||t_{12}|.$$

Second, we choose (possibly suboptimally) the phases of t_{11} and t_{21} so that $|c_{41}t_{11} + t_{21}|^2$ is minimized, i.e.,

$$t_{21} = -\frac{c_{41}}{|c_{41}|}|t_{21}|.$$

The argument is that what gives the dramatic gain from coherency is nulling, not beamforming.[5] Then (145) is

$$R_1 \le \log\left(1 + \frac{|t_{11}|^2 + |c_{32}|^2|t_{21}|^2 + 2\varphi|c_{32}||t_{11}||t_{21}| + A_1^2}{1 + |c_{32}|^2A_2^2}\right) \tag{146}$$

with

$$\varphi = -\frac{\mathrm{Re}\{c_{41}c_{32}\}}{|c_{41}||c_{32}|}. \tag{147}$$

Fix the value of R_1 between 0 and the maximum (given by the relay channel between nodes 1 and 3 with node 2 as relay node). For a given value of R_1 it is optimal to choose A_1 as small as possible, so A_1 is therefore also fixed through (139). Now fix A_2. From (146), we find that $|t_{11}|$ and $|t_{21}|$ should satisfy the equation

$$\begin{aligned} &|t_{11}|^2 + |c_{32}|^2|t_{21}|^2 + 2\varphi|c_{32}||t_{11}||t_{21}| \\ &\qquad = \left(2^{R_1} - 1\right)\left(1 + |c_{32}|^2A_2^2\right) - A_1^2. \end{aligned} \tag{148}$$

What remains is an optimization over A_1, A_2, and $|t_{21}|$ which can be done by a grid search.

While the solution for finite SNR requires numerical optimization, we can find a closed-form solution for the high-SNR offset, as follows.

Proposition 6: The high-SNR offset using "dirty-paper" coding is given by

$$a = \log\left(\left(|c_{41}||t_{12}| + |t_{22}|\right)^2\right) + \log\left(\frac{|c_{21}|^2}{|c_{41}|^2}\right) \tag{149}$$

[4]More precisely, it can create a copy of $Y_3[i]$ in (144) below by adding a linear combination of U_1^0 and U_2^0.

[5]This corresponds to ZF-DP coding in [35], which is shown to be near optimum in many cases.

where $|t_{12}|$ and $|t_{22}|$ satisfy

$$P_1 \geq |t_{12}|^2 + \frac{|c_{32}|^2|c_{21}|^2}{|c_{41}|^2|c_{12}|^2\left(1+|c_{41}|^2|c_{32}|^2+2\varphi|c_{41}||c_{32}|\right)} \times \left(|c_{41}||t_{12}|+|t_{22}|\right)^2 \quad (150)$$

$$P_2 \geq |t_{22}|^2 + \frac{|c_{32}|^2|c_{21}|^2}{|c_{12}|^2\left(1+|c_{41}|^2|c_{32}|^2+2\varphi|c_{41}||c_{32}|\right)} \times \left(|c_{41}||t_{12}|+|t_{22}|\right)^2; \quad (151)$$

furthermore, this high-SNR offset is achieved along the line $R_1 = R_2$.

Proof: To get a solution with multiplexing factor 1 for the sum rate $R_1 + R_2$, we must have $R_1, R_2 \sim \log(\sqrt{\text{SNR}})$ (this excludes solution where R_1 and R_2 increase at different rate with SNR, but such solutions are not true multisource solutions and are mostly suboptimal). From (139) and (140), it is seen that we must have $A_1^2, A_2^2 \sim \sqrt{\text{SNR}}$, and from (145) and (143), that $|t_{ij}|^2 \sim$ SNR. We therefore put $P_i = \sigma^{-2}\tilde{P}_i$, $\tilde{t}_{ij} = \sigma t_{ij}$, and $\tilde{A}_i = \sqrt{\sigma}A_i$, where $\tilde{P}_i, \tilde{t}_{ij}$, and $\tilde{A}_i$ are constants (or, to be more precise, converge toward constants for $\sigma^2 \to 0$), and let $\sigma^2 \to 0$ in the corresponding expressions.

First, from (143) it is seen that we must have $c_{41}t_{11}+t_{21}=0$; otherwise, R_1 would be bounded. Inserting $t_{21} = -c_{41}t_{11}$ in the rate bounds, we can now write the rate region as

$$R_1 \leq \log(1+|c_{21}|^2A_1^2) \quad (152)$$

$$R_2 \leq \log(1+|c_{12}|^2A_2^2) \quad (153)$$

$$R_1 \leq \log\left(1+\frac{|t_{11}|^2+|c_{41}|^2|c_{32}|^2|t_{11}|^2+2\varphi|c_{41}||c_{32}||t_{11}|^2}{1+|c_{32}|^2A_2^2} + \frac{A_1^2}{1+|c_{32}|^2A_2^2}\right) \quad (154)$$

$$R_2 \leq \log\left(1+\frac{\left(|t_{22}|+|c_{41}||t_{12}|\right)^2}{1+|c_{41}|^2A_1^2}+\frac{A_2^2}{1+|c_{41}|^2A_1^2}\right). \quad (155)$$

We will argue that without loss of generality we can assume that the two bounds for R_1 are equal and that the two bounds for R_2 are equal in the high-SNR region. Suppose that we have a solution where (152) is larger than (154). If we decrease A_1, the bound (152) clearly decreases. In the bound (154) the last term inside the log also decreases, but this is a bounded term, and it therefore does not influence the high-SNR limit. Thus, decreasing A_1 decreases the limit of (152) but either increases or has no influence on the limit of (154), and A_1 can therefore be decreased to make the two bounds equal. A similar argument can be used if we have a solution where (154) is larger than (152).

Equalizing the two bounds for R_1 and the two bounds for R_2, we get the equations

$$|c_{21}|^2A_1^2+|c_{32}|^2|c_{21}|^2A_1^2A_2^2 = |t_{11}|^2+|c_{41}|^2|c_{32}|^2|t_{11}|^2 + 2\varphi|c_{41}||c_{32}||t_{11}|^2+A_1^2 \quad (156)$$

$$|c_{12}|^2A_2^2+|c_{41}|^2|c_{12}|^2A_1^2A_2^2 = \left(|t_{22}|+|c_{41}||t_{12}|\right)^2+A_2^2. \quad (157)$$

We multiply these equations through with σ^{-2}, and take the limit $\sigma^2 \to 0$. Eliminating terms that have limit 0, we then end up with the equations

$$|c_{32}|^2|c_{21}|^2\tilde{A}_1^2\tilde{A}_2^2 = |\tilde{t}_{11}|^2+|c_{41}|^2|c_{32}|^2|\tilde{t}_{11}|^2 + 2\varphi|c_{41}||c_{32}||\tilde{t}_{11}|^2 \quad (158)$$

$$|c_{41}|^2|c_{12}|^2\tilde{A}_1^2\tilde{A}_2^2 = \left(|\tilde{t}_{22}|+|c_{41}||\tilde{t}_{12}|\right)^2. \quad (159)$$

From this we get

$$\frac{|\tilde{t}_{22}|+|c_{41}||\tilde{t}_{12}|}{|c_{41}||c_{12}|} = \frac{1}{|c_{32}||c_{21}|} \times\sqrt{1+|c_{41}|^2|c_{32}|^2+2\varphi|c_{41}||c_{32}|}|\tilde{t}_{11}|. \quad (160)$$

The high-SNR offset can now be calculated as

$$a = \lim_{\sigma^2\to 0}\Big(\log\left(1+|c_{21}|^2\sigma^{-1}\tilde{A}_1^2\right) + \log\left(1+|c_{12}|^2\sigma^{-1}\tilde{A}_2^2\right)-\log\left(\sigma^{-2}\right)\Big) \quad (161)$$

$$= \log\left(|c_{12}|^2|c_{21}|^2\tilde{A}_1^2\tilde{A}_2^2\right) \quad (162)$$

$$= \log\left(\left(|\tilde{t}_{22}|+|c_{41}||\tilde{t}_{12}|\right)^2\right)+\log\left(\frac{|c_{21}|^2}{|c_{41}|^2}\right). \quad (163)$$

Multiplying the power constraint (136) with σ^{-2} and taking the limit $\sigma^2 \to 0$ results in

$$|\tilde{t}_{11}|^2+|\tilde{t}_{12}|^2 \leq P_1$$
$$|\tilde{t}_{21}|^2+|\tilde{t}_{22}|^2 \leq P_2. \quad (164)$$

Using (160) and $\tilde{t}_{21} = -c_{41}\tilde{t}_{11}$ results in (150) and (151).

To see that the solution corresponds to the line $R_1 = R_2$, the easiest way seems to be to solve the problem again with the constraint $R_1 = R_2$, and see that it results in the same high-SNR offset. Since the calculations are similar we will not put the details here. □

It is easy to find closed-form expressions for $|t_{11}|$ and $|t_{21}|$ as functions of P_1 and P_2 (requires solving a second-order polynomial equation), but the resulting expressions are complicated and do not give much insight. Rather, it is instructive to compare the expression (149) with the expressions (130) and (132). The expressions (149), (130), and (132) all have a second log term which is approximately $\log\left(\frac{|c_{21}|^2}{|c_{41}|^2}\right)$—if $|c_{21}|^2 \gg |c_{41}|^2$ the extra 1 in the expressions have little influence. From the expressions (150) and (151) it can be seen that $|t_{12}|^2 \approx P_1$ and $|t_{22}|^2 \approx P_2$ if the second terms are small. This is the case, for example, if $|c_{32}| \ll 1$, i.e., weak interference. If so, the achievable high-SNR offset (149) is nearly equal to the upper bound, and thus characterizes capacity.

Now comparing the upper bounds with the result for no cooperation, Proposition 2, it can be seen that for strong interference, $|c_{41}| > 1$ the difference in the upper bound is the

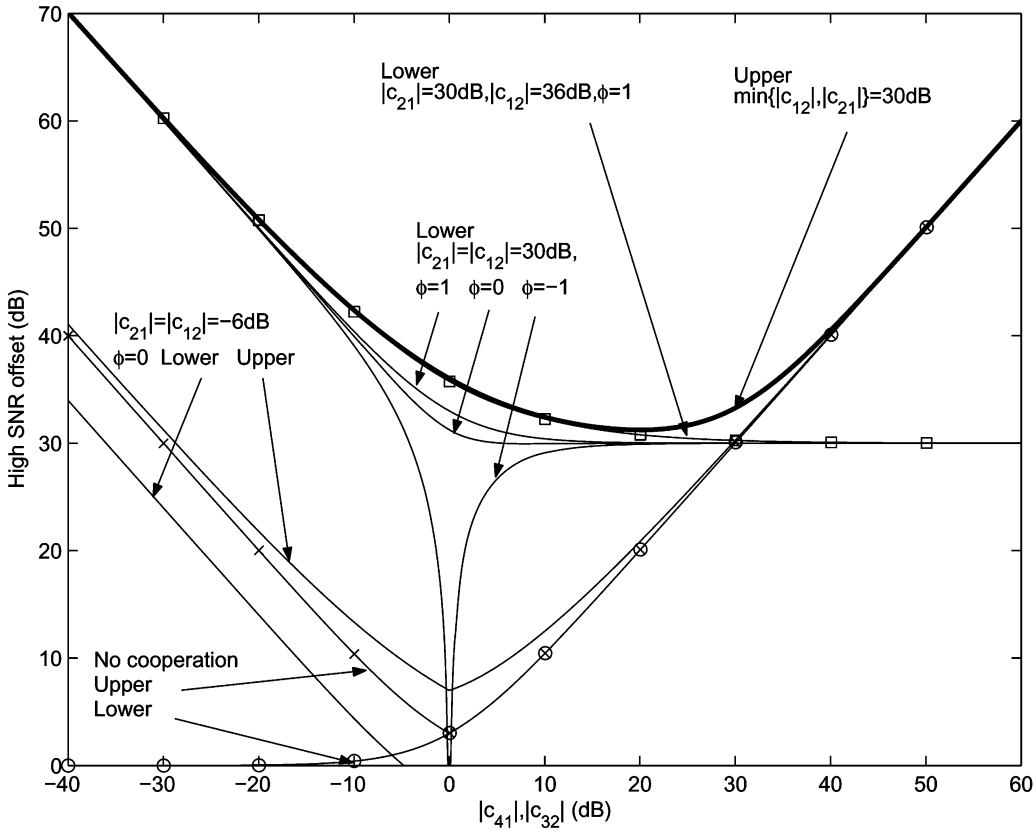

Fig. 8. High SNR offset for $|c_{32}|^2 = |c_{41}|^2$.

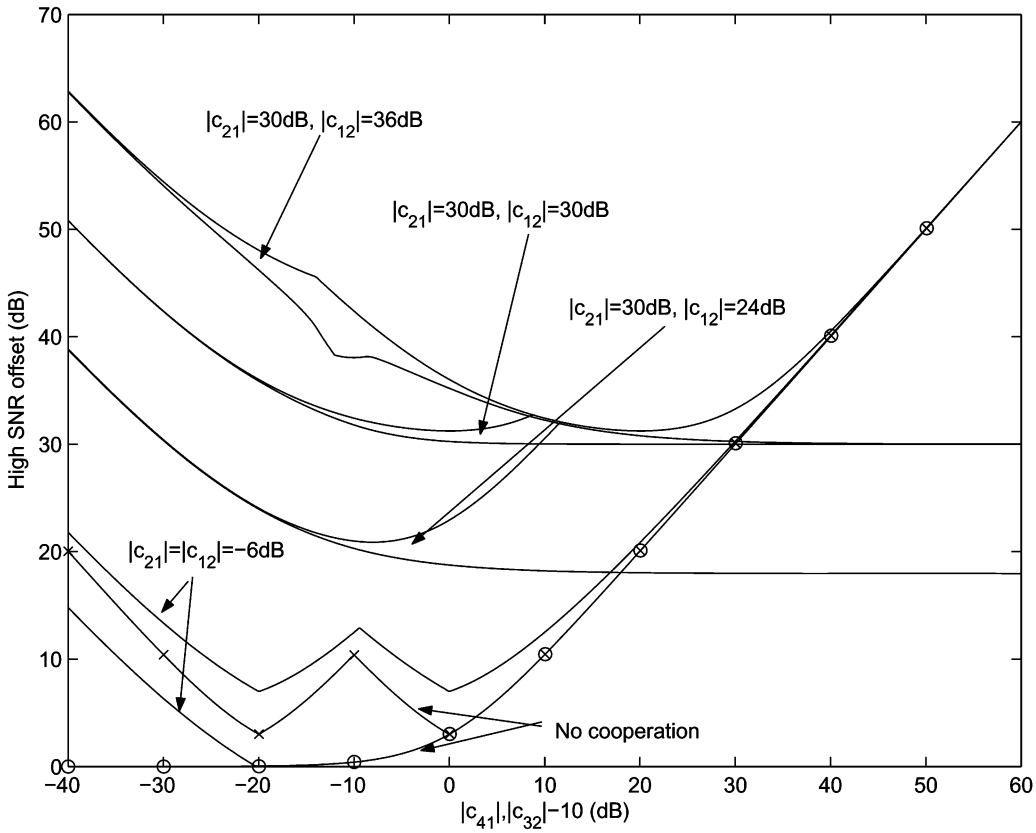

Fig. 9. High SNR offset for $|c_{32}|^2 = 100|c_{41}|^2$.

term $\log\left(\frac{|c_{21}|^2}{|c_{41}|^2}\right)$, and for weak interference $|c_{41}| < 1$ the term $\log\left(|c_{21}|^2\right)$. Thus, these terms characterize the gain from transmitter cooperation.

The above is only an approximate hand-waving type argument based on the form of the expressions, and we have therefore plotted the expressions in Figs. 8 and 9. A couple of

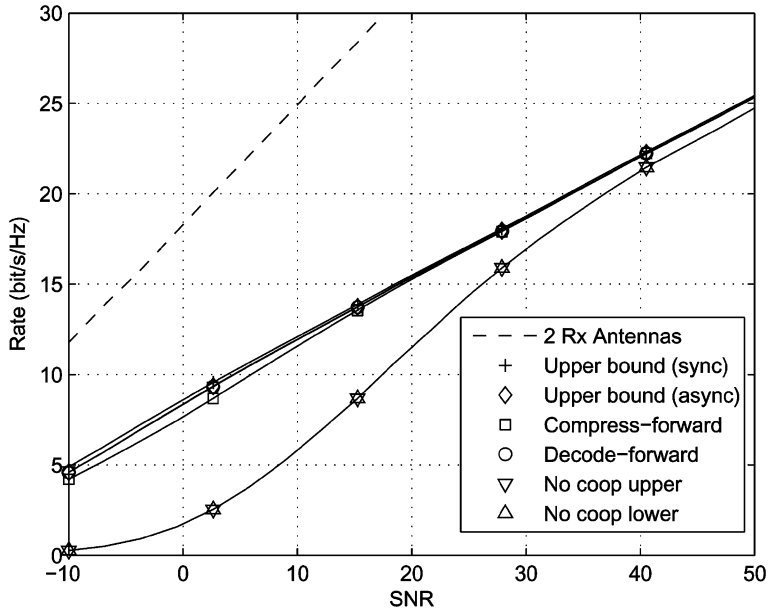

Fig. 10. Receiver cooperation: $E[|h_{43}|^2]P_3 = E[|h_{31}|^2]P_1+20$ dB, $E[|h_{41}|^2]P_1 = E[|h_{31}|^2]P_1+30$ dB.

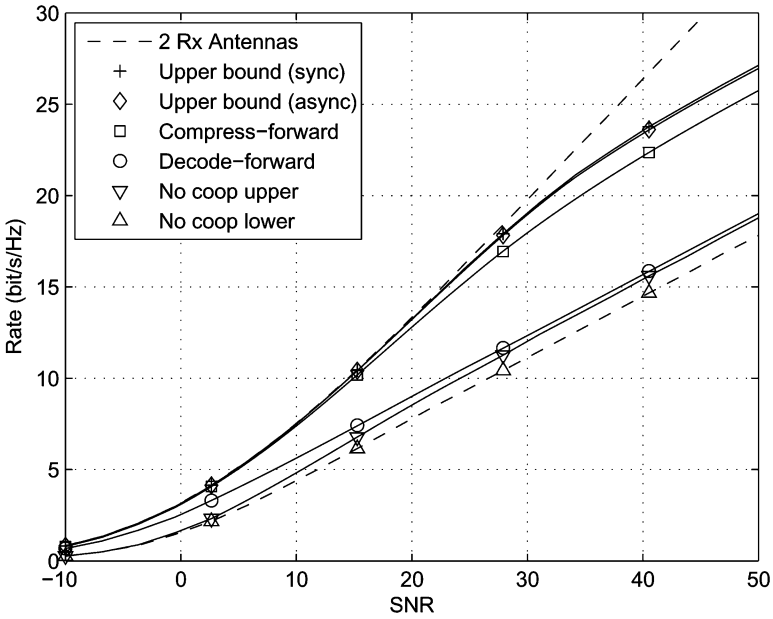

Fig. 11. Receiver cooperation: $E[|h_{43}|^2]P_3 = E[|h_{31}|^2]P_1+30$ dB, $E[|h_{41}|^2]P_1 = E[|h_{31}|^2]P_1+0$ dB.

thingsshould be noticed from these figures, also implicit in the expressions.

- Generally, upper and lower bounds for cooperation are close, although there are gaps for certain parameter values showing that better upper or lower bounds can still be developed.
- For strong interference, $|c_{32}|, |c_{41}| \gg 1$, there is no gain from transmitter cooperation. This shows that what is going on is very different from relaying, since is this region the relaying effect would be strongest. Thus, the gain from transmitter cooperation is due to interference avoidance; not enough to increase the multiplexing factor, but enough to increase the offset.
- For weak interference, $|c_{32}|, |c_{41}| \ll 1$, upper and lower bounds meet, and the gain from cooperation is given by $\min\{\log(|c_{21}|), \log(|c_{21}|)\}$ measured from the upper bound without cooperation, or

$$\min\left\{\log\left(\frac{|c_{12}|^2}{|c_{32}|^2}\right), \log\left(\frac{|c_{21}|^2}{|c_{41}|^2}\right)\right\}$$

from the best known noncooperative achievable rate.
- For weak interference, the achievable rate for no cooperation does not increase with decreasing interference, as opposed to the upper bound. This is because, as far as is known to the author, there is no way to take advantage of weak interference without cooperation. However, even when the link between the transmitters is weak (the curve for $|c_{12}| = |c_{21}| = -6$ dB) cooperation can compensate for weak interference.

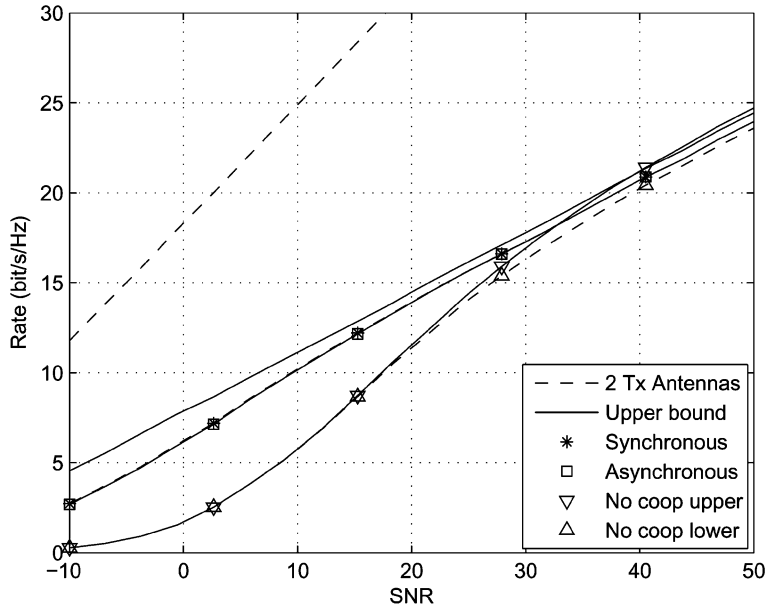

Fig. 12. Transmitter cooperation: $E[|h_{21}|^2]P_1 = E[|h_{31}|^2]P_1+20$ dB, $E[|h_{41}|^2]P_1 = E[|h_{31}|^2]P_1+30$ dB. The upper bound is for synchronous systems.

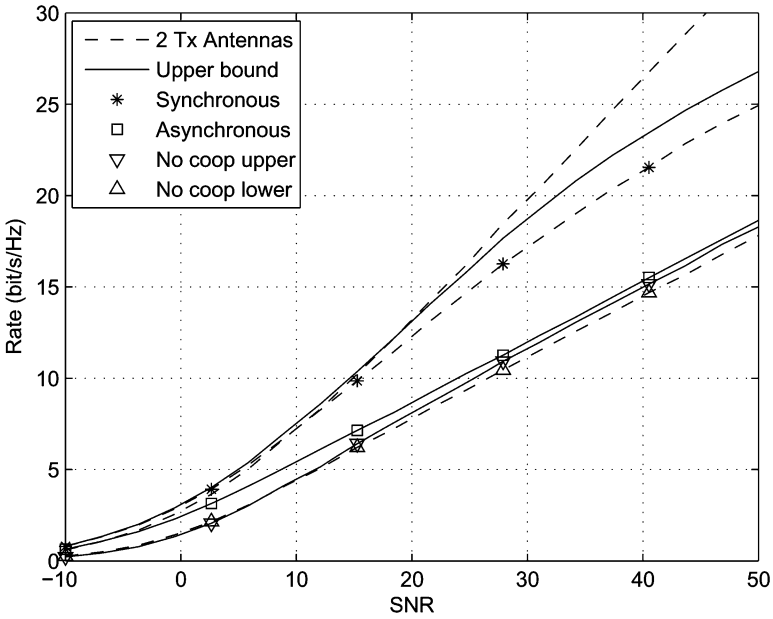

Fig. 13. Transmitter cooperation: $E[|h_{21}|^2]P_1 = E[|h_{31}|^2]P_1+30$ dB, $E[|h_{41}|^2]P_1 = E[|h_{31}|^2]P_1+0$ dB. The upper bound is for synchronous systems.

VII. Numerical Results

The various results on the high-SNR offset throughout the paper show analytically that the upper and lower bounds in general are close in the high-SNR regime, and gives a simple analytical characterization of the gain from cooperation. But it should not be forgotten that the bounds developed are also valid for finite SNR, and the behavior here is not necessarily the same as in the high-SNR regime. However, for finite SNR numerical evaluation of the bounds are needed to compare upper and lower bounds. We will here show a few typical numerical results.

The theoretical results are for fixed values of c_{ij}, and each set of values c_{ij} gives different results. To generate some representative numerical results we assume that all the channels between the nodes are independent Rayleigh-fading channels, i.e., in Fig. 1 all the h_{ij} are independent Gaussian. To generate different scenarios, we vary the average channel gains $E[|h_{ij}|^2]$ between different figures. The scenarios are symmetric in the sense that $E[|h_{31}|^2] = E[|h_{42}|^2]$ and $E[|h_{41}|^2] = E[|h_{32}|^2]$ and that all powers P_i are equal (in the nonnormalized model). The noise power $\sigma^2 = 1$. We use the received power on the direct link, $E[|h_{31}|^2]P_1$, as the SNR, and let the gains $E[|h_{41}|^2]P_1$ and $E[|h_{43}|^2]P_3$ be relative to the SNR.

As representative performance measure we use the sum rate $R_1 + R_2$, and we consider the average rate over the ensemble h_{ij}. Figs. 10–13 show the results.

In the high-SNR regime (i.e., SNR >30 dB), the results are as predicted by the high SNR analysis elsewhere in the paper. In the medium-SNR regime, the results, however, provide some new insights. First, when the cooperating nodes are close together, Figs. 11 and 13, the curves for cooperation initially follow the

two-antenna curves, i.e., cooperation does have a multiplexing factor of 2 defined in a heuristic fashion. Eventually, the multiplexing factor drops to 1, as predicted by the theory, and the gain over no cooperation is determined by the high-SNR offset. Secondly, even when the high SNR results predict no or a limited gain from cooperation, Fig. 12 and to some extent Fig. 10, in the medium-SNR regime there can still be a significant gain.

Another way to look at this is to notice that the gain from cooperation in the high- and medium-SNR regimes are for nearly opposite channel conditions: when the gains on the interlinks are much stronger than the interference links, Figs. 11 and 13, there is a gain in the high-SNR regime, but no gain in the low/medium-SNR regime. On the other hand, when the interference links are stronger than the interlinks Figs. 10 and 12, there is a gain in the low/medium-SNR regime, but not in the high-SNR regime. Furthermore, to get this latter gain, synchronization is not needed, neither for transmitter nor receiver cooperation.

VIII. Conclusion

We have derived upper and lower bounds for the capacity of a four-node cooperative diversity network, and used these to in particular characterize the gain from cooperation in the high-SNR regime. The results show that there is no multiplexing gain from either transmitter or receiver cooperation,[6] but there is an additive gain, a gain in the offset in the high-SNR regime.

The results makes it possible to characterize the gain from cooperation as a rule for thumb in a few words, at least in the high-SNR regime.

- Transmitter cooperation gives no gain for strong interference ($|c_{41}|, |c_{32}| \gg 1$), but for weak interference the gain is given by an extra term, $\min\{\log(|c_{21}|), \log(|c_{21}|)\}$, assuming there is a way to compensate for weak interference without cooperation, or

$$\min\left\{\log\left(\frac{|c_{12}|^2}{|c_{32}|^2}\right), \log\left(\frac{|c_{21}|^2}{|c_{41}|^2}\right)\right\}$$

  without such a way. To get a significant gain, transmitter synchronization is essential.
- Receiver cooperation gives a gain for both weak and strong inteference, and the gain is given by an extra term *inside* the log: $\log(\cdots + |c_{43}|^2 P_3)$ or $\log(\cdots + |c_{34}|^2 P_4)$ for asynchronous systems. Transmitter synchronization does not give a significant additional gain.

[6]This result has been extended to arbitrary cooperation in [36].

There are a number of interesting extension of this work that can be considered. First is the more realistic scenario when the nodes cannot operate in full duplex, but must use time-division duplex (TDD) or frequency-division duplex (FDD). In principle, the theoretical results here can easily be generalized to this model, but the whole problem ends up with a huge numerical optimization problem over time or frequency schedules, which is perhaps less interesting. Secondly, an extension to larger networks is attractive, but not straightforward.

Appendix A
Calculation of Achievable Rates for Receiver Cooperation

We will first derive the rates for compress–forward. Consider forward decoding at receiver 3 (cooperation last). For reference, we will repeat the received signals here

$$Y_3[i] = X_1(w_1[i]) + c_{32}X_2(w_2[i]) + c_{34}X_4[i] + Z_3[i] \tag{165}$$

$$Y_3[i+1] = X_1(w_1[i+1]) + c_{32}X_2(w_2[i+1]) + c_{34}X_4[i+1] + Z_3[i+1] \tag{166}$$

$$Y_4[i] = c_{41}X_1(w_1[i]) + X_2(w_2[i]) + c_{43}X_3[i] + Z_4[i] \tag{167}$$

$$Y_4[i+1] = c_{41}X_1(w_1[i+1]) + X_2(w_2[i+1]) + c_{43}X_3[i+1] + Z_4[i+1]. \tag{168}$$

Node 3 starts by decoding the channel code $X_4[i+1]$ from (166). It can do so if

$$R_4 \le \log\left(1 + \frac{|c_{34}|^2 P_4}{P_1 + |c_{32}|^2 P_2 + 1}\right) \tag{169}$$

as $X_1(w_1[i+1]) + c_{32}X_2(w_2[i+1])$ can be treated as part of the background Gaussian noise (a special case is the last block, where nodes 1 and 2 do not transmit; that can only decrease the probability of error). Next, node 3 decompresses $Y_4[i]$. In doing so, it has the side information $Y_3[i]$. Furthermore, it knows $X_3[i]$ so that this can be ignored in the calculations according to Corollary 1. Additionally, by the forward decoding assumption, it has already decoded $X_4[i]$. The Wyner–Ziv compression therefore operates on the virtual received signals

$$Y_3'[i] = X_1(w_1[i]) + c_{32}X_2(w_2[i]) + Z_3[i] \tag{170}$$

$$Y_4'[i] = c_{41}X_1(w_1[i]) + X_2(w_2[i]) + Z_4[i]. \tag{171}$$

According to Proposition 1, this is equivalent to node 3 having an antenna array that receives $(Y_3'[i], Y_4'[i] + Z_W)$, where Z_W has power given by (172) and (173) at the bottom of the page.

$$\begin{aligned}\sigma_w^2 &= \frac{E\left[|Y_4'|^2\right] E\left[|Y_3'|^2\right] - \left|E\left[Y_4' Y_3'^*\right]\right|^2}{(2^{R_4}-1)\, E\left[|Y_3'|^2\right]} \\ &= \frac{\left(|c_{41}|^2 P_1 + P_2 + 1\right)\left(P_1 + |c_{32}|^2 P_2 + 1\right) - |c_{41}P_1 + c_{32}^* P_2|^2}{(2^{R_4}-1)\left(P_1 + |c_{32}|^2 P_2 + 1\right)} \qquad (172) \\ &= \frac{|c_{41}^2| P_1 + P_2 + 1 + P_1 + |c_{32}|^2 P_2 + \left(|c_{32}|^2 |c_{41}|^2 - 2\mathrm{Re}\{c_{41}c_{32}\} + 1\right) P_1 P_2}{(2^{R_4}-1)\left(P_1 + |c_{32}|^2 P_2 + 1\right)}. \qquad (173)\end{aligned}$$

$$\sigma_w^2 = \frac{|c_{41}^2|P_1 + P_2 + 1 + P_1 + |c_{32}|^2 P_2 + \left(|c_{32}|^2|c_{41}|^2 - 2\mathrm{Re}\{c_{41}c_{32}\} + 1\right) P_1 P_2}{|c_{34}|^2 P_4}. \tag{174}$$

$$R_1 = \log \begin{vmatrix} P_1 + |c_{32}|^2 P_2 + 1 & c_{41}P_1 + c_{32}^* P_2 \\ c_{41}^* P_1 + c_{32} P_2 & |c_{41}^2|P_1 + P_2 + 1 + \sigma_w^2 \end{vmatrix} - \log \begin{vmatrix} |c_{32}|^2 P_2 + 1 & c_{32}^* P_2 \\ c_{32} P_2 & P_2 + 1 + \sigma_w^2 \end{vmatrix} \tag{175}$$

$$= \log \left(1 + \frac{\left(|c_{41}|^2 + 1 + \sigma_w^2\right) P_1 + \left(|c_{32}|^2|c_{41}|^2 - 2\mathrm{Re}\{c_{41}c_{32}\} + 1\right) P_1 P_2}{\left(|c_{32}|^2 + |c_{32}|^2\sigma_w^2 + 1\right) P_2 + 1 + \sigma_w^2} \right) \tag{176}$$

Inserting the upper bound expression (169) for R_4 we then get (174), at the top of the page.

Node 3 now has two alternatives: it can decode $w_1[i]$ individually, considering the signal $X_2(w_2[i])$ as interference, or it can decode $w_1[i]$ and $w_2[i]$ jointly. Individual decoding gives the bound on R_1, given in (175) and (176) also at the top of the page, whereas there is no bound on R_2. This gives row 2 in Table I

Joint decoding gives the bounds on the rates R_1 and R_2 in (177)–(179) at the bottom of the page. There are a symmetric set of rate bounds at node 4. This gives row 3 in Table I

Consider instead backward decoding (cooperation first). The assumption is now that node 3 has successfully decoded $w_1[i+1]$ and $w_2[i+1]$ It then forms

$$\begin{aligned} Y_3'[i+1] &= Y_3[i+1] - X_1(w_1[i+1]) - c_{32}X_2(w_2[i+1]) \\ &= c_{34}X_4[i+1] + Z_3[i], \end{aligned} \tag{180}$$

it then decodes the channel code of $X_4[i+1]$, which it can do if

$$R_4 \le \log\left(1 + |c_{34}|^2 P_4\right). \tag{181}$$

It then decompresses $Y_4[i]$. According to Proposition 1, the system is equivalent to a system where node 3 has two antennas that receive the signals

$$\begin{bmatrix} X_1(w_1[i]) + c_{32}X_2(w_2[i]) + c_{34}X_4[i] + Z_3[i] \\ X_2(w_2[i]) + c_{41}X_1(w_1[i]) + Z_4[i] + Z_W \end{bmatrix} \tag{182}$$

where Z_W is compression noise with a power shown in (183), also at the bottom of the page. From this received signal, it now decodes $w_1[i]$ and $w_2[i]$. Notice that $X_4[i]$ acts as Gaussian interference, and with calculation similar to (177)–(179) we get the rate bounds in row 5 in Table I.

We next derive achievable rates for decode–forward. First, consider the cooperation first case, Fig. 5. The received signals are

$$\begin{aligned} Y_3[i] &= X_1(w_1[i]) + c_{32}X_2(w_2[i]) \\ &\quad + c_{34}X_4(w_1[i-1]) + Z_3[i] \end{aligned} \tag{184}$$

$$\begin{aligned} Y_4[i] &= X_2(w_2[i]) + c_{41}X_1(w_1[i]) \\ &\quad + c_{43}X_3(w_2[i-1]) + Z_4[i]. \end{aligned} \tag{185}$$

Consider decoding at node 3 at time instant i, and suppose node 3 has decoded $w_1[i-2]$ and $w_2[i-1]$. By subtracting the corresponding signals from Y_3 it can then form

$$\begin{aligned} Y_3'[i-1] &= Y_3[i-1] - c_{32}X_2(w_2[i-1]) \\ &\quad - c_{34}X_4(w_1[i-2]) \\ &= X_1(w_1[i-1]) + Z_3[i-1] \end{aligned} \tag{186}$$

using the signals $Y_3'[i-1]$ and $Y_3[i]$; it then decodes $w_1[i-1]$ and $w_2[i]$ jointly considering $X_1(w_1[i])$ as Gaussian noise. According to Section III-B we then get the following rate bounds:

$$\begin{aligned} R_1 &\le \log(1 + P_1) + \log\left(1 + \frac{|c_{34}|^2 P_4}{1 + P_1}\right) \\ &= \log\left(1 + P_1 + |c_{34}|^2 P_4\right) \end{aligned} \tag{187}$$

$$R_2 \le \log\left(1 + \frac{|c_{32}|^2 P_2}{1 + P_1}\right) \tag{188}$$

$$\begin{aligned} R_1 &\le \log \begin{vmatrix} P_1 + 1 & c_{41}P_1 \\ c_{41}^* P_1 & |c_{41}^2|P_1 + 1 + \sigma_w^2 \end{vmatrix} - \log \begin{vmatrix} 1 & 0 \\ 0 & 1 + \sigma_w^2 \end{vmatrix} \\ &= \log\left(1 + P_1 + \frac{|c_{41}|^2 P_1}{1 + \sigma_w^2}\right) \end{aligned} \tag{177}$$

$$R_2 \le \log\left(1 + |c_{32}|^2 P_2 + \frac{P_2}{1 + \sigma_w^2}\right) \tag{178}$$

$$\begin{aligned} R_1 + R_2 &\le \log \begin{vmatrix} P_1 + |c_{32}|^2 P_2 + 1 & c_{41}P_1 + c_{32}^* P_2 \\ c_{41}^* P_1 + c_{32} P_2 & |c_{41}^2|P_1 + P_2 + 1 + \sigma_w^2 \end{vmatrix} - \log \begin{vmatrix} 1 & 0 \\ 0 & 1 + \sigma_w^2 \end{vmatrix} \\ &= \log\left(1 + P_1 + \frac{|c_{41}|^2 P_1}{1 + \sigma_w^2} + |c_{32}|^2 P_2 + \frac{P_2}{1 + \sigma_w^2} + \frac{\left(|c_{32}|^2|c_{41}|^2 - 2\mathrm{Re}\{c_{41}c_{32}\} + 1\right) P_1 P_2}{1 + \sigma_w^2}\right). \end{aligned} \tag{179}$$

$$\sigma_w^2 = \frac{|c_{41}|^2(1 + |c_{34}|^2 P_4)P_1 + (1 + |c_{34}|^2 P_4)P_2 + 1 + |c_{34}|^2 P_4 + P_1 + |c_{32}|^2 P_2}{|c_{43}|^2 P_3 \left(P_1 + |c_{32}|^2 P_2 + |c_{34}|^2 P_4 + 1\right)} + \frac{\left(|c_{32}|^2|c_{41}|^2 - 2\mathrm{Re}\{c_{41}c_{32}\} + 1\right) P_1 P_2}{|c_{43}|^2 P_3 \left(P_1 + |c_{32}|^2 P_2 + |c_{34}|^2 P_4 + 1\right)}. \tag{183}$$

$$R_1+R_2 \le \log(1+P_1)+\log\left(1+\frac{|c_{32}|^2P_2}{1+P_1}+\frac{|c_{34}|^2P_4}{1+P_1}\right) = \log\left(1+P_1+|c_{32}|^2P_2+|c_{34}|^2P_4\right). \quad (189)$$

If node 4 uses the same kind of decoding, we get a symmetric set of rate bounds, which is row 1 in Table II.

When node 3 only decodes its own message, the transmission of node 2 acts as interference, and it therefore has the rate bound in row 2, column 2, in Table II. Node 4 does not receive any assistance from node 3, but still has to do joint decoding to forward to node 3, and it therefore has an ordinary MAC capacity bound [37, Sec. 14.3.6], which is row 2, column 3, in Table II.

Consider instead cooperation last, Fig. 6. Node 3 waits with decoding and forwarding w_2 until it has received the forwarded information from node 4. The received signal is

$$Y_3[i] = X_1(w_1[i]) + c_{32}X_2(w_2[i]) + c_{34}X_4(w_1[i-2]) + Z_3[i] \quad (190)$$

$$Y_4[i] = X_2(w_2[i]) + c_{41}X_1(w_1[i]) + c_{43}X_3(w_2[i-1]) + Z_4[i]. \quad (191)$$

Consider decoding at node 3 in block i, and suppose node 3 has decoded $w_2[i-2]$ and $w_1[i-4]$. By subtracting the corresponding signals from $Y_3[i-2]$ it can then form

$$Y_3'[i-2] = Y_3[i-2] - c_{32}X_2(w_2[i-2]) - c_{34}X_4(w_1[i-4]) = X_1(w_1[i-2]) + Z_3[i-2] \quad (192)$$

using the signals $Y_3'[i-2]$ and $Y_3[i]$ it then decodes $w_1[i-2]$ and $w_2[i]$ jointly. This is the same problem as considered above, just with larger delay, and the decoding is therefore possible if (R_1,R_2) satisfy (187)–(189).

Now consider decoding at node 4 during block i, and suppose node 4 has decoded $w_2[i-2]$. By subtracting the corresponding signal from Y_4 it can then form

$$Y_4'[i-1] = Y_4[i-1] - c_{43}X_3(w_2[i-2]) = X_2(w_2[i-1]) + c_{41}X_1(w_1[i-1]) + Z_4[i-1] \quad (193)$$

using the signals $Y_4'[i-1]$ and $Y_4[i]$ it then decodes $w_2[i-1]$ and $w_1[i-1]$ jointly. According to Section III-B, this is possible if the rates (R_1,R_2) satisfy

$$R_1 \le \log\left(1+|c_{41}|^2P_1\right) \quad (194)$$

$$R_2 \le \log(1+P_2) + \log\left(1+\frac{|c_{43}|^2P_3}{1+|c_{41}|^2P_1+P_2}\right) \quad (195)$$

$$R_1+R_2 \le \log\left(1+|c_{41}|^2P_1+P_2\right) + \log\left(1+\frac{|c_{43}|^2P_3}{1+|c_{41}|^2P_1+P_2}\right) = \log\left(1+|c_{41}|^2P_1+P_2+|c_{43}|^2P_3\right) \quad (196)$$

which gives row 4 in Table II.

Appendix B
Calculation of Achievable Rates for Transmitter Cooperation

We consider at first joint decoding at both nodes 3 and 4. The transmission is

$$\begin{bmatrix}X_1[i]\\X_2[i]\end{bmatrix} = \begin{bmatrix}A_1 & 0\\0 & A_2\end{bmatrix}\begin{bmatrix}U_1(w_1[i],w_1[i-1],w_2[i-1])\\U_2(w_2[i],w_1[i-1],w_2[i-1])\end{bmatrix} \quad (197)$$

where each of the codewords U_1 and U_2 are i.i.d. Gaussian codewords of power 1, encoded using multiplexed coding, Section III-A, and $A_i=\sqrt{P_i}$. Nodes 1 and 2 use forward decoding. Consider decoding at node 1, with received signal

$$Y_1[i] = c_{12}A_2U_2(w_2[i],w_1[i-1],w_2[i-1]) + Z_1[i]. \quad (198)$$

Node 1 knows $w_1[i-1]$, and by the forward decoding assumption it has decoded $w_2[i-1]$ correctly. It can then decode $w_2[i]$ from $Y_1[i]$ if $R_2 \le \log(1+|c_{12}|^2P_2)$. Thus, R_1 and R_2 must satisfy (133) and (134).

Now consider backward decoding at node 3, with joint decoding. Node 3 receives

$$Y_3[i] = A_1U_1(w_1[i],w_1[i-1],w_2[i-1]) + c_{32}A_2U_2(w_2[i],w_1[i-1],w_2[i-1]) + Z_3[i]. \quad (199)$$

By assumption, mode 3 has decoded $w_1[i]$ and $w_2[i]$. A standard argument using joint typicality (cf. [37, Sec. 14.3.1], in particular equation (14.71)) now shows node 3 can decode $w_1[i-1]$ and $w_2[i-1]$ if

$$R_1+R_2 \le \log(1+P_1+|c_{32}|^2P_2) \quad (200)$$

and similarly for node 4. This gives row 1 in Table III.

If only one node 2 forward the transmission is

$$\begin{bmatrix}X_1[i]\\X_2[i]\end{bmatrix} = \begin{bmatrix}A_1 & 0\\0 & A_2\end{bmatrix}\begin{bmatrix}U_1(w_1[i],w_1[i-1])\\U_2(w_2[i],w_1[i-1],w_2[i-1])\end{bmatrix}. \quad (201)$$

With similar decoding as above, this gives the rate bound in row 2 in Table III.

Now consider instead individual decoding at nodes 3 and 4, i.e., each node only decodes its own message. The transmission is

$$\begin{bmatrix}X_1[i]\\X_2[i]\end{bmatrix} = \begin{bmatrix}A_1 & 0\\0 & A_2\end{bmatrix}\begin{bmatrix}U_1(w_1[i])\\U_2(w_2[i])\end{bmatrix} + \begin{bmatrix}\tilde{A}_1 & 0\\0 & \tilde{A}_2\end{bmatrix}\begin{bmatrix}U_1^0(w_2[i-1])\\U_2^0(w_1[i-1])\end{bmatrix} \quad (202)$$

where each of U_1, U_2, U_1^0, and U_2^0 are independent Gaussian i.i.d. codebooks of power 1, and the constants A satisfy

$$A_1^2+\tilde{A}_1^2 \le P_1 \quad (203)$$

$$A_2^2+\tilde{A}_2^2 \le P_2. \quad (204)$$

These constants can be (numerically) optimized to maximize the rate region. Using parallel Gaussian channel arguments, Section III-B, this gives

$$R_1 \le \log\left(1+\frac{A_1^2}{1+\tilde{A}_1^2+|c_{32}|^2A_2^2}\right) + \log\left(1+\frac{|c_{32}|^2\tilde{A}_2^2}{1+A_1^2+\tilde{A}_1^2+|c_{32}|^2A_2^2}\right) \quad (205)$$

$$= \log\left(1+\frac{A_1^2+|c_{32}|^2\tilde{A}_2^2}{1+\tilde{A}_1^2+|c_{32}|^2A_2^2}\right) \quad (206)$$

with a similar bound for R_2. This gives row 3 in Table III.

If only node 2 forward, the transmission is

$$\begin{bmatrix}X_1[i]\\X_2[i]\end{bmatrix} = \begin{bmatrix}A_1 & 0\\0 & A_2\end{bmatrix}\begin{bmatrix}U_1(w_1[i])\\U_2(w_2[i])\end{bmatrix} + \begin{bmatrix}0 & 0\\0 & \tilde{A}_2\end{bmatrix}\begin{bmatrix}0\\U_2^0(w_1[i-1])\end{bmatrix} \quad (207)$$

which gives the rate bounds in row 4 in Table III.

For combined decoding, with joint decoding at node 3 and individual decoding at node 4, the transmission is

$$\begin{bmatrix}X_1[i]\\X_2[i]\end{bmatrix} = \begin{bmatrix}A_1 & 0\\0 & A_2\end{bmatrix}\begin{bmatrix}U_1(w_1[i],w_1[i-1],w_2[i-1])\\U_2(w_2[i],w_2[i-1])\end{bmatrix} + \begin{bmatrix}\tilde{A}_1 & 0\\0 & \tilde{A}_2\end{bmatrix}\begin{bmatrix}U_1^0(w_2[i-1])\\U_2^0(w_1[i-1],w_2[i-1])\end{bmatrix}. \quad (208)$$

We then get the rate bounds (133) and (134) and

$$R_1 \le \log\left(1+A_1^2+|c_{32}|^2\tilde{A}_2^2\right) \quad (209)$$

$$R_2 \le \log\left(1+\frac{A_2^2+|c_{41}|^2\tilde{A}_1^2}{1+\tilde{A}_2^2+|c_{41}|^2A_1^2}\right) \quad (210)$$

$$R_1+R_2 \le \log\left(1+P_1+|c_{32}|^2P_2\right) \quad (211)$$

which is row 5 in Table III.

If only node 2 forward, the transmission is

$$\begin{bmatrix}X_1[i]\\X_2[i]\end{bmatrix} = \begin{bmatrix}A_1 & 0\\0 & A_2\end{bmatrix}\begin{bmatrix}U_1(w_1[i],w_1[i-1],w_2[i-1])\\U_2(w_2[i])\end{bmatrix} + \begin{bmatrix}0 & 0\\0 & \tilde{A}_2\end{bmatrix}\begin{bmatrix}0\\U_2^0(w_1[i-1],w_2[i-1])\end{bmatrix} \quad (212)$$

which gives row 6 in Table III.

Finally, if only node 1 forward, the transmission is

$$\begin{bmatrix}X_1[i]\\X_2[i]\end{bmatrix} = \begin{bmatrix}A_1 & 0\\0 & A_2\end{bmatrix}\begin{bmatrix}U_1(w_1[i],w_1[i-1],w_2[i-1])\\U_2(w_2[i],w_2[i-1])\end{bmatrix} + \begin{bmatrix}\tilde{A}_1 & 0\\0 & 0\end{bmatrix}\begin{bmatrix}U_1^0(w_2[i-1])\\0\end{bmatrix} \quad (213)$$

which gives row 7 in Table III.

ACKNOWLEDGMENT

The author thanks the anonymous reviewers for their detailed review that improved this paper considerably. He is also grateful to Aria Nosratinia, Nihar Jindal, and Momin Uppal for constructive feedback.

REFERENCES

[1] C. Heegard, J. Coffey, S. Gummadi, P. Murphy, R. Provencio, E. Rossin, S. Schrum, and M. Shoemake, "High-performance wireless ethernet," *IEEE Commun. Mag.*, vol. 39, no. 11, pp. 64–73, Nov. 2001.

[2] A. Doufexi, S. Armour, M. Butler, A. Nix, D. Bull, and J. McGeehan, "A comparison of the HIPERLAN/2 and IEEE 802.11a wireless LAN standards," *IEEE Commun. Mag.*, vol. 40, no. 5, pp. 172–180, May 2002.

[3] K. Negus, "HomeRF: Wireless networking for the connected home," *IEEE Personal Commun.*, pp. 20–27, Feb. 2000.

[4] J. Haartsen, "The bluetooth radio system," *IEEE Personal Commun.*, pp. 28–36, Feb. 2000.

[5] G. Pottie and W. Kaiwer, "Wireless integrated network sensors," *Commun. Assoc. Comp. Mach.*, vol. 43, no. 5, pp. 551–558, 2000.

[6] P. Gupta and P. Kumar, "The capacity of wireless networks," *IEEE Trans. Inf. Theory*, vol. 46, no. 2, pp. 388–404, Mar. 2000.

[7] G. Foschini, "Layered space-time architecture for wireless communication in a fading environment when using multi-element antennas," *Bell Labs Tech. J.*, pp. 41–59, 1996.

[8] İ. E. Telatar, "Capacity of multi-antenna Gaussian channels," *Europ. Trans. Telecommun.*, vol. 10, no. 6, pp. 585–595, Nov./Dec. 1999.

[9] W. Kuo and M. Fitz, "Design and analysis of transmitter diversity using intentional frequency offset for wireless communications," *IEEE Trans. Veh. Technol.*, vol. 46, no. 6, pp. 871–881, Nov. 1997.

[10] V. Tarokh, N. Seshadri, and A. Calderbank, "Spacetime codes for high data rate wireless communication: Performance criterion and code construction," *IEEE Trans. Inf. Theory*, vol. 44, no. 2, pp. 744–765, Mar. 1998.

[11] S. Alamouti, "A simple transmit diversity technique for wireless communications," *IEEE J. Sel. Areas Commun.*, vol. 16, no. 10, pp. 1451–1458, Oct. 1998.

[12] A. Sendonaris, E. Erkip, and B. Aazhang, "Increasing uplink capacity via user cooperation diversity," in *Proc. IEEE Int. Symp. Information Theory*, Cambridge, MA, Aug. 1998, p. 156.

[13] ——, "User cooperation diversity-part I: System description," *IEEE Trans. Commun.*, vol. 51, no. 11, pp. 1927–1938, Nov. 2003.

[14] ——, "User cooperation diversity-Part II: Implementation aspects and performance analysis," *IEEE Trans. Commun.*, vol. 51, no. 11, pp. 1939–1948, Nov. 2003.

[15] A. Stefanov and E. Erkip, "Cooperative information transmission in wireless networks," in *Proc. Asian-European ITW 2002*, Breisach, Germany, Jun. 2002.

[16] J. Laneman and G. Wornell, "Exploiting distributed spatial diversity in wireless networks," in *Proc. 38th Allerton Conf. Communication, Control, and Computing*, Monticello, IL, Oct. 2000.

[17] ——, "Energy-efficient antenna sharing and relaying for wireless networks," in *Proc. IEEE Wireless Communications and Networking Conf.: WCNC'00*, Chicago, IL, Sep. 2000.

[18] J. N. Laneman, D. N. C. Tse, and G. W. Wornell, "Cooperative diversity in wireless networks, efficient protocols, and outage behavior," *IEEE Trans. Inf. Theory*, vol. 50, no. 12, pp. 3062–3080, Dec. 2004.

[19] J. Laneman and G. Wornell, "Distributed space–time-coded protocols for exploiting cooperative diversity in wireless networks," *IEEE Trans. Inf. Theory*, vol. 49, no. 10, pp. 2415–2425, Oct. 2003.

[20] J. Laneman, E. Martinian, G. Wornell, J. Apostolopoulos, and J. Wee, "Comparing application-and physical-layer approaches to diversity on wireless channels," in *Proc. IEEE Int. Conf. Communications: ICC'03*, 2003.

[21] F. Willems and E. van der Meulen, "The discrete memoryless multiple-access channel with cribbing encoders," *IEEE Trans. Inf. Theory*, vol. IT-31, no. 3, pp. 313–327, May 1985.

[22] F. Willems, "The discrete memoryless multi-access channel with partially cooperating encoders," *IEEE Trans. Inf. Theory*, vol. IT-29, no. 3, pp. 441–445, May 1983.

[23] T. Cover and A. El Gamal, "Capacity theorems for the relay channel," *IEEE Trans. Inf. Theory*, vol. IT-25, no. 5, pp. 572–584, Sep. 1979.

[24] A. Høst-Madsen and J. Zhang, "Capacity bounds and power allocation for wireless relay channels," *IEEE Trans. Inf. Theory*, vol. 51, no. 6, pp. 2020–2040, Jun. 2005.

[25] G. Kramer, M. Gastpar, and P. Gupta, "Cooperative strategies and capacity theorems for relay networks," *IEEE Trans. Inf. Theory*, vol. 51, no. 9, pp. 3037–3063, Sep. 2005.

[26] P. Gupta and P. Kumar, "Towards an information theory of large networks: An achievable rate region," in *Proc. IEEE Int. Symp. Information Theory*, Washington, DC, Jun. 2001, p. 159.

[27] ——, "Towards and information theory of large networks: An achievable rate region," *IEEE Trans. Inf. Theory*, vol. 49, no. 8, pp. 1877–1894, Aug. 2003.

[28] A. Høst-Madsen, "On the capacity of cooperative diversity in slow fading channels," in *Proc. 40th Annu. Allerton Conf. Communication, Control, and Computing*, Monticello, IL, Oct. 2002.

[29] ——, "A new achievable rate for cooperative diversity based on generalized writing on dirty paper," in *Proc. IEEE Int. Symp. Information Theory*, Yokohama, Japan, Jun./Jul. 2003.

[30] ——, "Upper and lower bounds for channel capacity of asynchronous cooperative diversity networks," in *Proc. 38th Annu. Conf. Information Sciences and Systems*, Princeton, NJ, Mar. 2004.

[31] L. Zheng and D. N. C. Tse, "Diversity and multiplexing: A fundamental tradeoff in multiple-antenna channels," *IEEE Trans. Inf. Theory*, vol. 49, no. 5, pp. 1073–1096, May 2003.

[32] A. Lozano, A. Tulino, and S. Verdú, "High-SNR power offset in multiantenna communication," *IEEE Trans. Inf. Theory*, vol. 51, no. 12, pp. 4134–4151, Dec. 2005.

[33] S. Shamai (Shitz) and S. Verdú, "The impact of frequency-flat fading on the spectral efficiency of cdma," *IEEE Trans. Inf. Theory*, vol. 47, no. 4, pp. 1302–1327, May 2001.

[34] N. Jindal, "High SNR analysis of MIMO broadcast channels," in *Proc. IEEE Int. Symp. Information Theory*, Adelaide, Australia, Sep. 2005, pp. 2310–2314.

[35] G. Caire and S. Shamai (Shitz), "On the achievable throughput of a multiple-antenna Gaussian broadcast channel," *IEEE Trans. Inf. Theory*, vol. 49, no. 7, pp. 1691–1706, Jul. 2003.

[36] A. Høst-Madsen and A. Nosratinia, "The multiplexing gain of wireless networks," in *Proc. IEEE Int. Symp. Information Theory*, Adelaide, Australia, Sep. 2005, pp. 2065–2069.

[37] T. Cover and J. Thomas, *Information Theory*. New York: Wiley, 1991.

[38] A. Carleial, "Interference channels," *IEEE Trans. Inf. Theory*, vol. IT-24, no. 1, pp. 60–70, Jan. 1978.

[39] W. Shiroma and M. P. D. Lisio, "Quasioptical circuits," in *Wiley Encyclopedia of Electrical and Electronics Engineering*. New York: Wiley, 1999, pp. 523–533.

[40] C. Zeng, F. Kuhlmann, and A. Buzo, "Achievability proof of some multiuser channel coding theorems using backward decoding," *IEEE Trans. Inf. Theory*, vol. 35, no. 6, pp. 1160–1165, Nov. 1989.

[41] M. C. Valenti and B. Zhao, "Capacity approaching distributed turbo codes for the relay channel," in *Proc 57th IEEE Semiannual Vehicular Technology Conf: VTC'03-Spring*, Jeju, Korea, Apr. 2003.

[42] A. Wyner and J. Ziv, "The rate-distortion function for source coding with side information at the decoder," *IEEE Trans. Inf. Theory*, vol. IT-22, no. 1, pp. 1–10, Jan. 1976.

[43] A. Wyner, "The rate-distortion function for source coding with side information at the decoder-II: General sources," *Inf. Contr.*, vol. 38, pp. 60–80, 1978.

[44] M. Costa, "Writing on dirty paper," *IEEE Trans. Inf. Theory*, vol. IT-29, no. 3, pp. 439–441, May 1983.

[45] H. Weingarten, Y. Steinberg, and S. Shamai (Shitz), "The capacity region of the Gaussian MIMO broadcast channel," in *Proc. 38th Annu.Conf. Information Sciences and Systems*, Princeton, NJ, Mar. 2004.

[46] T. Iian and K. Kobayashi, "A new achievable rate region for the interference channel," *IEEE Trans. Inf. Theory*, vol. IT-27, no. 1, pp. 49–60, Jan. 1981.

[47] H. Sato, "The capacity of the Gaussian interference channel under strong interference," *IEEE Trans. Inf. Theory*, vol. IT-27, no. 6, pp. 786–788, Nov. 1981.

[48] M. Costa, "On the Gaussian interference channel," *IEEE Trans. Inf. Theory*, vol. IT-31, no. 5, pp. 607–615, Sep. 1985.

[49] G. Kramer, "Genie-aided outer bounds on the capacity of interference channels," in *Proc. IEEE Int. Symp. Information Theory*, Washington, DC, Jun. 2001, p. 103.

[50] ——, "Outer bounds on the capacity of Gaussian interference channels," *IEEE Trans. Inf. Theory*, vol. 50, no. 3, pp. 581–586, Mar. 2004.

[51] N. Blachman, "The convolution inequality for entropy powers," *IEEE Trans. Info. Theory*, vol. IT-11, no. 2, pp. 267–271, Apr. 1965.

[52] P. Bergmans, "A simple converse for broadcast channels with additive white Gaussian noise," *IEEE Trans. Inf. Theory*, vol. IT-20, no. 2, pp. 279–280, Mar. 1974.